UNIVERSITY OF MANITOBA

Numerical and experimental studies on the localization of a small crack with optimized spatial wavelet analysis and windowing

by

Amir Ghanbari Mardasi

A thesis submitted to the Faculty of Graduate Studies of

The University of Manitoba

in partial fulfillment of the requirements for the degree of

MASTER OF SCIENCE

Department of Mechanical Engineering

University of Manitoba

Winnipeg, Manitoba, Canada

ABSTRACT

In this thesis, a high sensitive spatial wavelet-based crack localization technique is presented on a cracked beam structure. Due to the crack existence in the beam structure, a perturbation/slop singularity is induced in the displacement profile. Spatial wavelet transformation works as a magnifier to amplify the small perturbation signal at the crack location to detect and localize the damage. This technique is studied both theoretically and experimentally. Theoretical model and vibration analysis considering the crack effect are first proposed and performed in MATLAB based on the Timoshenko beam model. Wavelet scale in spatial wavelet transformation is optimized to enhance crack detection sensitivity. As the outcome of the simulation, optimal ranges are obtained for wavelet scale factor. The experimental part of thesis is based on the obtained ranges. The experiment is then carried out on a cracked cantilever beam subjected to a certain displacement at the free end. The profile of a deflected aluminum cantilever beam is obtained for both intact and cracked beams by a high-resolution laser profile sensor. Gabor wavelet transformation is applied on the subtraction of intact and cracked data sets. To improve crack localization sensitivity, scale factor optimization process in spatial wavelet transformation is conducted. Furthermore, to detect the possible crack very close to the measurement boundaries, wavelet transformation edge effect, which is large values of wavelet coefficient around the measurement boundaries, is efficiently reduced by introducing different windowing functions. The result shows that a small crack with depth of 10% of the beam height can be localized with a clear perturbation. Moreover, a perturbation caused by a crack 0.85 mm away from one end of the measurement range, which is covered by wavelet transform edge effect, emerges by applying proper window functions.

ACKNOWLEDGEMENTS

I would first like to thank my thesis supervisor Dr. Nan Wu. The door to his office was always open whenever I ran into a trouble spot or had a question regarding my research. He gave me freedom to bring up new ideas, and steered me in the right direction whenever he thought it was essential.

I would also like to thank my colleagues in our lab and my friends for the great time we spent together in the last two years.

The last, but certainly not the least, I would like to express my very profound gratitude and love to my family for providing me with unfailing support and continuous encouragement throughout my years of study. Specifically my mother whom I owe all that I have in my life.

My sincere thanks to all of you,

Amir Ghanbari Mardasi.

Dedicated to my mother...

TABLE OF CONTENTS

LIST OF TABLES

LIST OF FIGURES

LIST OF SYMBOLS

ω	Lateral displacement of the beam
ρ	Density of the beam material
A	Cross-section area of the beam
E	Elastic modulus of the beam material
G	Shear modulus of the beam material
I	Second moment of area of the beam
k	Timoshenko shear coefficient
$\emptyset$	Slope of the deflection curve
L	Beam length
h	Beam height
b	Beam width
d	Crack depth
e	Crack location
Kt	Stiffness of rotational spring

1 INTRODUCTION

1.1 PROBLEM STATEMENT

Nowadays damage detection and localization have been common topics among researchers to enhance the stability, durability and safety of engineering structures [1]. Detection of the structural damages at an early stage is a crucial aspect of decision making about the regularly maintenance and repair works to extend structure lifetime. In the engineering applications, cantilever is considered as one the most important employed components. As a result, many researches have been performed for the damage detection in cantilever structures. Damage is a general word and in the most mechanical and civil applications crack is known as the specific kind of damage. There are different kinds of crack with various causes. They may be fatigue cracks or due to mechanical defects or may be cracks inside the material, which have been created during manufacturing process. Many efforts have been carried out in this area because of variety of cracks, and their causes, and also attention to this point that crack is a serious threat to machine performance. Failure to detect the faults has various consequences, and sometimes may lead to a fatal disaster. A quick and proper crack detection can prevent dangerous consequences. To ensure structural stability and reliability, it is essential to accomplish long-term, mid-term and short-term health monitoring of the structure during its service life.

A wide range of damage identification methods have been used in the mechanical and civil engineering researches during last decades. Most of these methods are based on the fact that a damage changes the physical properties of the structure such as stiffness, mass, and damping ratio

[2]. In the Vibration-based damage identification, these alterations and their effects on the modal properties of the structure such as mode shapes and natural frequencies have been investigated. Investigation of the change in the natural frequency was the earliest vibration-based method to identify the damage [3]–[9]. Natural frequency change is considered as a sign to show defects in the structure. In this technique, comparison between measured frequencies of intact and damaged structures leads to determination of damage properties [10], [11]. Analysis of changes in the mode shape and its derivatives is another method of damage identification [6]. Using space domain signal such as mode shape and deflection as a feature to detect the damage has some advantages over the natural frequency-based method [12]–[14]. Space domain signals can reveal local information which makes them more sensitive to local defects [7]. Moreover, these signals are less affected by environmental factors, such as temperature variations, as compared to the natural frequencies of a structure. Dynamically measured flexibility matrix is another tool to estimate changes in the static behavior of the structure [15]. Moreover, analyzing the dynamic and static space domain signals of structures, which can be obtained by various kinds of sensors (piezoelectric, strain gauge, optical sensor and so on) has been emerged as another way of experimentally identifying damages in the structures. Analysis of the output signals of the sensors is an important issue during the identification procedure. Several mathematical tools have been utilized to analyze these signals. Fourier transform is one of the first tools which have been employed to show the damage effect in the signal. However, this transformation was not found as a powerful tool providing detailed information about particularly non-stationary signals. In the other word, all information which varies with time cannot be found during signal processing with Fourier transform. Fast Fourier transform, and wavelet transform have been developed in order to

solve the limitations of the Fourier transform and are considered as the next generation of tools for signal processing. Over last decades, wavelet transformation has been a popular tool among researchers to analyze the signals to ease the damage detection procedure. The popularity of these tools is due to their ability to identify even small perturbation in signals. Thus, wavelet transforms reveal detailed information of the signal to make the damage detection feasible. All these various methods have been employed to improve the damage identification procedure. Next section includes some of the most important simulation and experimental studies in this area.

1.2 Previous Studies

1.2.1 Simulation Studies

Many simulation works have been conducted in this area, for instance, Surace and Ruotolo developed the theory of wavelets and their applications [16]. They used the wavelet transform to analyze vibration response signals of a cracked beam. The measured signal was obtained by an accelerometer mounted on the beam. Results proved that presented method was more sensitive in identifying relatively small cracks than methods based on the shift in resonance frequencies. Liew and Wang presented the application of wavelet transformation in the space domain to identify a crack in the structure [17]. A cracked simply supported beam has been mathematically modeled and spatial wavelet transform has been used to identify the crack in the beam structure. Eventually, based on the results, wavelet-based method eased the crack identification procedure compared to the traditional method (natural frequency change). Wang and Deng performed a study on the crack detection in the plate and beam structures by using Haar and Gabor wavelet families [18]. In simulations, they considered both dynamic and static loading conditions on the structures. Both

wavelet families successfully achieved the damage identification. This research was an interesting start point of using spatial wavelet transform for damage identification in structural diagnosis and structural health monitoring. Jaiswal and Pande carried out numerical studies for purpose of damage detection in a beam structure by applying spatial wavelet transform to mode shape curvatures [19]. The authors investigated the crack depths larger than 17% of the beam height and cracks were at the distance greater than 17% of the beam length from one end of wavelet analysis range. A wavelet-based technique has been presented for the crack detection in beam structures [20], [21]. In these two simulation studies, Timoshenko beam theory has been used to model the beam structure. They conducted spatial wavelet analysis (Gabor family) for the mode shapes of a beam in both single and multiple cracks conditions. Although, results showed that this technique worked for cracks larger than 10% of the beam thickness, these studies were limited for cracks located between 10% and 85% of the beam length, then failed to detect cracks closer to the measurement boundaries. A wavelet-based analytical study has been carried out for singly cracked beams in [22]. Static deflection profile has been used as the input of wavelet analysis. A discontinuity in the wavelet coefficients plot was considered as the crack effect in the signal. This paper included a parametric study regarding varying load intensity, length of the beam, and moment of inertia. This investigation included crack depths from 10% to 60% of the beam height, and crack positions from 30% to 70% of the beam length. Based on this study it has been concluded that wavelet coefficient values along the beam length are related to directly proportional to the location, and dimensions of damage, intensity of the load, and beam dimensions. Zhong and Oyadiji proposed a wavelet-based approach for small crack identification in beam-like structures [23]. This broad investigation contained cracks with different sizes and positions on a simply

supported beam structure in both single and multi-crack conditions. This study was based on differences between two sets of wavelet coefficients data, which were obtained by applying stationary wavelet transform to the mode shapes of the cracked and intact beam structures. The first and second mode shapes of the structure were analyzed in order to have a broad conclusion. It has been concluded that the proposed approach is able to identify a crack with depth of 4% of the beam height. To reach this goal in the real application a very detailed and accurate mode shape signal is needed which is considered as a significant limitation.

Previous simulation studies show that wavelet based damage detection methods can detect crack depths larger than 4% of the structure (Beam or plate) thickness. Furthermore, the closest crack to the signal boundary, which has been successfully detected, is located with distance of 10% of the signal length from the signal boundary. The mentioned simulation studies show the fact that the wavelet based damage identification methods have an important limitation that cracks located very close to the measurement boundaries have not been detected because of large wavelet coefficients around the boundaries.

1.2.2 Experimental Studies

In the case of practical applications, experimental studies are needed verifying the results from the simulation studies. Xu, Radzieński, Ostachowicz, and Cao conducted numerical and experimental studies on damage detection in plates using wavelet transform [24]. They made a notch with depth of 50% of the Plate thickness around the middle of the plate then the operating deflection shapes of the plate were measured by a laser vibrometer. Afterward, two-dimensional directional Gaussian wavelet transforms were employed in order to analyze the spatial signal of the plate structure. According to the results, Damage detection was successfully carried out for a notch

located around the middle and with depth of larger than 50% of the plate thickness. Rucka and Wilde conducted simulation and experimental studies for localization of a damage in a cantilever beam [25]. Static displacement of the cantilever beam was obtained by a digital camera then image processing was the next step to give the desired number of data points in the signal. Wavelet transform was applied to the static displacement to enlarge the crack effect in the signal. Results of this study showed the capability of this wavelet-based method for localization of a crack with depth of 35% of the beam height. This paper did not cover the investigation of cracks located close to the measurement boundaries. Wu and Wang did experimental studies on damage detection of a beam structure with wavelet transform [26]. They used a high-resolution laser to obtain the deflection profile of a cracked aluminum cantilever beam subjected to a certain displacement at its free end. De-noise techniques have been introduced to make the detection more efficient. The smoothed static profile of the cracked beam has been analyzed with Gabor wavelet to identify the crack with depth of 26% of the beam thickness. A singularity at the crack location in the wavelet coefficients along the measurement area causes a successful detection. Using the same method, Wang and Wu also achieved the detection of a delamination in a beam structure by using Gabor wavelet transform on the static displacement of the beam structure [27]. In the both studies, the crack and delamination were located around the middle of measurement area. Rucka worked on wavelet-based damage detection technique on a cantilever beam with a single notch [28]. He presented experimental and numerical analysis of damage detection based on higher order modes. The experimental results for detection of the notch with depth of 20% of the beam height showed a clear perturbation at notch location. However, for depths smaller than 20% of beam height, the results were not reliable since they were noisy. In this study, cracks located at different positions

have been investigated with different scale factor in wavelet analysis. However, the edge effect in wavelet analysis and methods to reduce it have not been studied. Wavelet transform has been used to analyze the mode shape signal of a beam structure in [29], [30]. The mode shape signal was obtained by embedded accelometers on the beam structure. In these papers, theoretical and experimental studies were conducted on different crack positions and depths. The experimental studies were based on the crack depths larger than 20% of the beam height. Furthermore, only cracks located between 25% and 75% of the beam length were investigated. For the mentioned crack sizes and positions, damage identification has been successfully carried out. Reddy and Swarnamani performed numerical and experimental studies on a wavelet-based damage detection and localization method for a plate structure [31]. The mode shapes and strain energy data of the structure have been analyzed in this paper. Experimental part of this work only showed successful detection of damage with depth larger than 15% of the plate thickness. Damages in the vicinity of the spatial signal boundaries were not analyzed and the studied damage is around the middle of the beam.

Although many efforts have been devoted to detecting and localizing small cracks by using wavelet transform. Still identification of crack depths smaller than 15% of the beam height has not been achieved experimentally. Moreover, identification process for the cracks, close to the signal boundaries, is still a problem blocking the application of spatial wavelet transformation to some cases of damage detection because of edge effect with large wavelet coefficient values in the vicinity of measurement boundaries in the wavelet analysis. In the previous researches, some methods for edge effect reduction have been tried and studied [19], [29], [30]. However, there is

no clear experimental result showing that cracks around the analysis boundaries can be detected after edge effect reduction.

1.3 Research Objectives

This thesis presents numerical and experimental studies for detection and localization of small cracks in a beam structure. According to aforementioned limitations in the previous performed studies in the damage identification area, two main objectives are defined in this research. (1) Localization of a small crack (depth<=10% of the beam height) with optimization of spatial wavelet algorism; and (2) detection of a small crack very close to the signal boundary after edge effect reduction by applying proper windowing functions. To achieve the defined goals in this research, at first some simulation studies are performed helping to guide the spatial wavelet algorism optimization, and then experimental studies are carried out so as to the results of simulations.

1.4 Thesis Organization

The organization of this thesis is such that, it is primarily based on two research papers which have been prepared during the M. Sc. Study (the two papers are given in the Appendix). The presented thesis includes four chapters: introduction, theoretical background and methodology, simulation studies, experimental studies, and a final chapter covers the conclusions and future works.

In the introduction chapter, the importance of this research is firstly presented followed by a literature survey in simulation and experimental areas. The objectives of this study are then clearly stated regarding the lack of some important investigations in this field of research.

The research methodology is subsequently presented in chapter two. The beam structure modeling equations are explained in detail, and the software and hardware used to solve the model for simulations are introduced. Moreover, in this chapter, the mathematical tool for signal analysis is introduced in detail.

After that, the findings of this research are presented in the chapters 3, and 4. The chapter 3 includes all the simulation studies' results, procedure and discussion. The obtained results from the experimental studies which verify the simulation results are presented in the chapter 4.

This study ends up with the conclusion and future works. The last chapter covers the main findings of the thesis, and based on the findings and experiences from the works done of this thesis, some suggestions for future works are given in order to improve the wavelet-based damage identification procedure.

2 THEORETICAL BACKGROUND AND METHODOLOGY

2.1 INTRODUCTION

Beam structures are considered as the most employed components in the engineering applications[32], [33]. Theoretical modeling of beam structures is based on three major theories.The equations of the motion of a beam structure are derived according to the Euler–Bernoulli, Rayleigh, and Timoshenko theories [34], [35]. According to the conditions and application of different structures, one of the theories is more appropriate and accurate for modeling of the structure. The most common and simplest theory for the beam structures is the Euler-Bernoulli because of simplifying assumptions considered inside of that. In this theory, the shear deformation of the beam and the rotary inertia effect are neglected which are considered as the appropriate assumptions when the beam is thin enough or subjected to a small displacement. The Rayleigh theory considers rotary inertia effect; however, this theory neglects the shear deformation in the structure. The third theory called Timoshenko considers both rotary inertia and shear deformation effects in the motion of the structure which makes this theory the most accurate one for beam modeling specially for thick beams or beams subjected to a large deflection [35], [36]. To have a better understanding of the differences between these three theories, their equations are presented as following:

Euler Bernoulli Theory

$$EI\frac{\partial^4\omega}{\partial x^4} + \rho A\frac{\partial^2\omega}{\partial t^2} = 0 \tag{2-1}$$

Rayleigh Theory

$$EI\frac{\partial^4\omega}{\partial x^4}+\ \rho A\frac{\partial^2\omega}{\partial t^2}-\rho I\frac{\partial^4\omega}{\partial x^2\partial t^2}=0 \tag{2-2}$$

Timoshenko Theory

$$EI\frac{\partial^4\omega}{\partial x^4}+\ \rho A\frac{\partial^2\omega}{\partial t^2}-\rho I\frac{\partial^4\omega}{\partial x^2\partial t^2}\ -\ \frac{\rho EI}{kG}\frac{\partial^4\omega}{\partial x^2\partial t^2}+\ \frac{\rho^2 I}{kG}\frac{\partial^4\omega}{\partial t^4}=0 \tag{2-3}$$

where ω is the lateral displacement, ρ is the density of the beam material, A is the cross-section area, E is the elastic modulus, G is the shear modulus, I is the second moment of area, k is called the Timoshenko shear coefficient that depends on the beam geometry (mostly =5/6 for a rectangular section)[20].

The first two terms in equation (2-3) are the same as those in the Eular-Bernouli theory. The third one represents the effect of rotary inertia, which is same as the third term in the Rayleigh theory. The last two terms in this equation involve kG in the denominators denote the effect of shear deformation. In this study, the theoretical model of the beam structure is based on the dynamic Timoshenko theory equations in the free vibration case.

2.2 THEORETICAL MODEL

In this section a cantilever beam with a through width crack is mathematically modeled. The schematic view of this cracked beam is shown in Figure 2-1. The Dimensions of the beam are mentioned in Table 2-1. Timoshenko equations for free vibration case as the start point of modeling procedure are as follows[34]:

$$-kAG\frac{\partial^2\omega}{\partial x^2}+kAG\frac{\partial\emptyset}{\partial x}+\ \rho A\frac{\partial^2\omega}{\partial t^2}=0, \tag{2-4}$$

$$-EI\frac{\partial^2 \emptyset}{\partial x^2} - kAG\frac{\partial \omega}{\partial x} + kAG\,\emptyset + \rho I\frac{\partial^2 \emptyset}{\partial t^2} = 0, \tag{2-5}$$

where $\emptyset$ is the slope of the deflection curve, and ω is the lateral displacement. Table 2-2 shows the material properties of the beam under study.

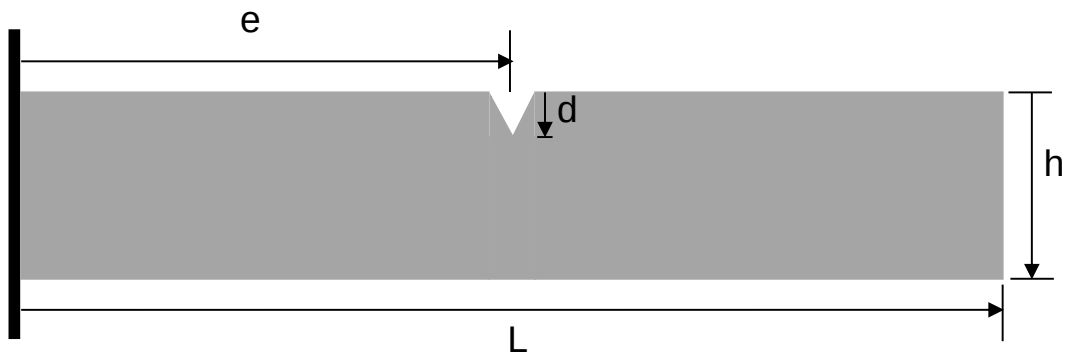

(a)

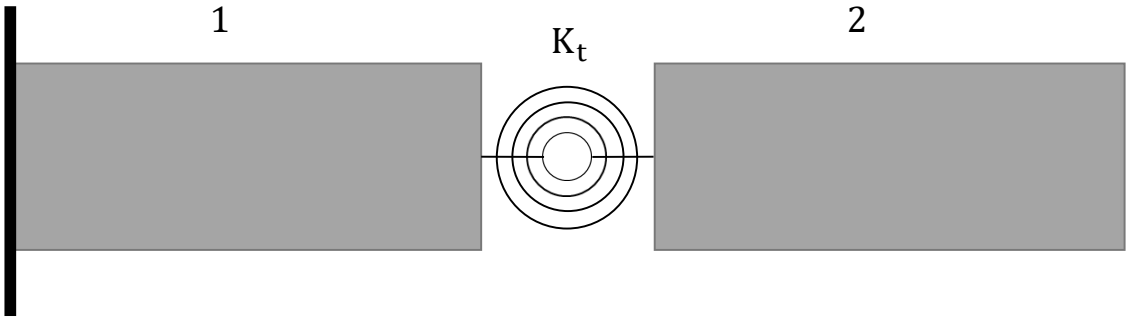

(b)

Figure 2-1 (a) Schematic of a cantilever beam with a through width crack. (b) Torsion spring representing the crack

Table 2-1 Beam dimensions

Symbol	Description	Quantity
L	Length	1 m
h	Height	0.1 m
b	Width	0.05 m

Table 2-2 Beam material properties

Symbol	Description	Quantity
ρ	Density of the beam material	7870 kg/m^3
E	Elastic modulus	210 Gpa
G	Shear modulus	79 Gpa

Free vibration solution can be obtained by using the separation of variables method. The $\omega(x,t)$and $\emptyset(x,t)$ are assumed as follows:

$$\omega(x,t) = W(x).e^{i\omega n.t} \ , \tag{2-6}$$

$$\emptyset(x,t) = P(x).e^{i\omega n.t} \ , \tag{2-7}$$

where ωn is the natural frequency of the structure. By substitution of equations (2-6) and (2-7) to (2-4) and (2-5):

$$-kAG\,\frac{d^2W(x)}{dx^2} + kAG\,\frac{dP(x)}{dx} - \rho A\omega n^2\,W(x) = 0 \tag{2-8}$$

$$-EI\,\frac{d^2P(x)}{dx^2} - kAG\,\frac{dW(x)}{dx} + kAG\,P(x) - \rho I\omega n^2\,P(x) = 0 \tag{2-9}$$

$W(x)$ and $P(x)$ are assumed as:

$$W(x) = C1.\,e^{a.x/L}\ , \tag{2-10}$$

$$P(x) = C2.\,e^{a.x/L}\ , \tag{2-11}$$

where L is the Beam length. After Substitution of equations (2-10) and (2-11) to (2-8) and (2-9):

$$\left(-kAG\,\frac{a^2}{L^2} - \rho A\omega n^2\right).C1 + \left(kAG\,\frac{a}{L}\right).C2 = 0 \tag{2-12}$$

$$\left(-kAG\,\frac{a}{L}\right).C1 + \left(-EI\,\frac{a^2}{L^2} + kAG - \rho I\omega n^2\right).C2 = 0 \tag{2-13}$$

To have a nontrivial solution of the constants $C1$ and $C2$, the determinant of their coefficients in equations (2-11) and (2-12) is set equal to zero:

$$a^4 + \left[\omega n^2L^2\left(\frac{\rho}{E} + \frac{\rho}{kG}\right)\right].a^2 + \left[\omega n^2L^4\left(\frac{\omega n^2\rho^2}{kGE} - \frac{\rho A}{EI}\right)\right] = 0 \tag{2-14}$$

The roots of equation (2-14) are given by:

$$a = \pm\left[-\frac{a1}{2} \pm \left(\left(\frac{a1}{2}\right)^2 - a2\right)^{\frac{1}{2}}\right]^{\frac{1}{2}}, \tag{2-15}$$

where:

$$a1 = \omega n^2 L^2 \rho\left(\frac{1}{E} + \frac{1}{kG}\right) \tag{2-16}$$

$$a2 = \omega n^2 L^4 \rho\left(\frac{\omega n^2 \rho}{kGE} - \frac{A}{EI}\right) \tag{2-17}$$

Four obtained values for a are employed to express $W(x)$ and $P(x)$ in the form of trigonometric and hyperbolic functions along the beam length. The model has two sections because of the defined crack at position of e on the beam structure.

For 0 < x < e (Crack position):

$$W1(x) = A1.\cosh\left(D1.\frac{x}{L}\right) + A2.\sinh\left(D1.\frac{x}{L}\right) + A3.\cos\left(D2.\frac{x}{L}\right) + A4.\sin\left(D2.\frac{x}{L}\right) \tag{2-18a}$$

$$P1(x) = m1.A1\sinh\left(D1.\frac{x}{L}\right) + m1.A2\cosh\left(D1.\frac{x}{L}\right) + m2.A3.\sin\left(D2.\frac{x}{L}\right) - m2.A4\cos\left(D2.\frac{x}{L}\right) \tag{2-18b}$$

For e < x < L:

$$W2(x) = A5.\cosh\left(D1.\frac{x}{L}\right) + A6.\sinh\left(D1.\frac{x}{L}\right) + A7.\cos\left(D2.\frac{x}{L}\right) + A8.\sin\left(D2.\frac{x}{L}\right) \tag{2-19a}$$

$$P2(x) = m1.A5\sinh\left(D1.\frac{x}{L}\right) + m1.A6\cosh\left(D1.\frac{x}{L}\right) + m2.A7\sin\left(D2.\frac{x}{L}\right) - m2.A8\cos\left(D2.\frac{x}{L}\right) \tag{2-19b}$$

where:

$$D1 = (-\frac{a1}{2} + ((\left(\frac{a1}{2}\right)^2 - a2)^{\frac{1}{2}})^{\frac{1}{2}} \quad (2\text{-}20)$$

$$D2 = (\frac{a1}{2} + ((\left(\frac{a1}{2}\right)^2 - a2)^{\frac{1}{2}})^{\frac{1}{2}} \quad (2\text{-}21)$$

$$m1 = \frac{(kGD1^2 + L^2\rho wn^2)}{LkGD1} \quad (2\text{-}22)$$

$$m2 = \frac{(-kGD2^2 + L^2\rho wn^2)}{LkGD2} \quad (2\text{-}23)$$

Two boundary conditions at the fixed end and two at the free end of the beam are as follows:

$$at\ x = 0 \qquad W1 = 0\ ,\ P1 = 0 \quad (2\text{-}24a)$$

$$at\ x = 1 \qquad \frac{dP2}{dx} = 0,\ \frac{dW2}{dx} - P2 = 0 \quad (2\text{-}24b)$$

At the crack position, the continuity of displacement, moment, and shear force are expressed in the following forms:

$$at\ x = e \qquad W1 = W2, \quad \frac{dP1}{dx} = \frac{dP2}{dx}\ , \quad P1 - \frac{dW1}{dx} = P2 - \frac{dW2}{dx} \quad (2\text{-}24c)$$

The slope fluctuation at the crack position is given by [37]:

$$P1 + \frac{EI}{KtL}.\frac{dP1}{dx} = P2 \quad (2\text{-}24d)$$

where Kt is the stiffness of rotational spring, which is calculated as follows:

$$Kt = \frac{bh^2E}{72\pi\left(\frac{d}{h}\right)^2 q(\frac{d}{h})} \tag{2-25}$$

where:

$$q\left(\frac{d}{h}\right) = 0.6384 - 1.035\left(\frac{d}{h}\right) + 3.7201\left(\frac{d}{h}\right)^2 - 5.1773\left(\frac{d}{h}\right)^3 + 7.553\left(\frac{d}{h}\right)^4 - 7.332\left(\frac{d}{h}\right)^5 + 2.4909\left(\frac{d}{h}\right)^6 \tag{2-26}$$

After applying eight boundary conditions, characteristic matrix is obtained in the page 19. For a nontrivial solution of A1, A2, A3, A4, A5, A6, A7, and A8 the determinant of their coefficients matrix must be zero. Expanding the determinant gives the frequency equation. The roots of this equation give the natural frequencies of the structure. Consequently, the mode shapes of the beam structure can be obtained. Figure 2-2 shows the first three mode shapes of the studied cantilever beam with a crack in the middle. According to this figure, no clear induced perturbation in the mode shapes of the cracked beam leads to investigation of the mode shape signal with a mathematical tool. In this research wavelet transform is the chosen tool for the signal analysis, which is explained in the next section.

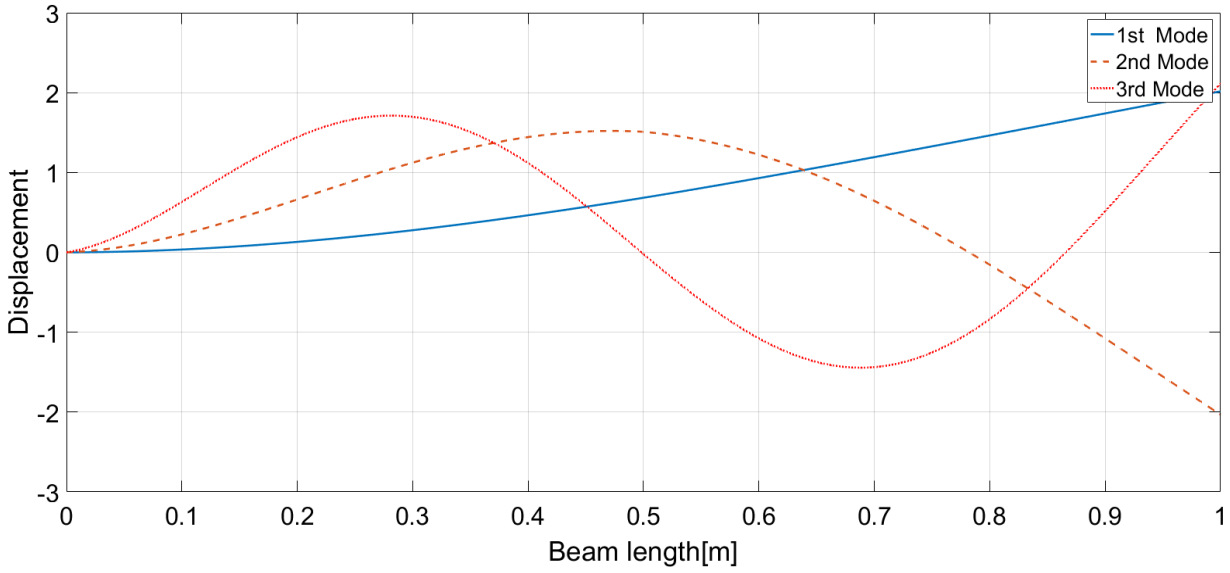

Figure 2-2 First three mode shapes of the cracked cantilever beam

$$
\begin{bmatrix}
1 & 0 & 1 & 0 \\
0 & m1 & 0 & -m2 \\
0 & 0 & 0 & 0 \\
0 & 0 & 0 & 0 \\
\cosh(e.D1) & \sinh(e.D1) & \cos(e.D2) & \sin(e.D2) \\
m1D1\cosh(e.D1) & m1D1\sinh(e.D1) & m2D2\cos(e.D2) & m2D2\sin(e.D2) \\
(m1-D1)\sinh(e.D1) & (m1-D1)\cosh(e.D1) & (m2+D2)\sin(e.D2) & -(m2+D2)\cos(e.D2) \\
m1\sinh(e.D1)+(\frac{EI}{KtL})m1D1\cosh(e.D1) & m1\cosh(e.D1)+(\frac{EI}{KtL})m1D1\sinh(e.D1) & m2\sin(e.D2)+\left(\frac{EI}{KtL}\right)m1D2\cos(e.D2) & -m2\cos(e.D2)+\left(\frac{EI}{KtL}\right)m2D2\sin(e.D2)
\end{bmatrix}
\begin{bmatrix}
0 & 0 & 0 & 0 \\
0 & 0 & 0 & 0 \\
m1D1\cosh(D1) & m1D1\sinh(D1) & m2D2\cos(D2) & m2D2\sin(D2) \\
(D1-m1)\sinh(D1) & (D1-m1)\cosh(D1) & -(m2+D2)\sin(D2) & (m2+D2)\cos(D2) \\
-\cosh(e.D1) & -\sinh(e.D1) & -\cos(e.D2) & \sin(e.D2) \\
-m1D1\cosh(e.D1) & -m1D1\sinh(e.D1) & -m2D2\cos(e.D2) & -m2D2\sin(e.D2) \\
(D1-m1)\sinh(e.D1) & (D1-m1)\cosh(e.D1) & -(m2+D2)\sin(e.D2) & (m2+D2)\cos(e.D2) \\
-m1\sinh(e.D1) & -m1\cosh(e.D1) & -m2\sin(e.D2) & m2\cos(e.D2)
\end{bmatrix}
\begin{bmatrix} A1 \\ A2 \\ A3 \\ A4 \\ A5 \\ A6 \\ A7 \\ A8 \end{bmatrix}
=
\begin{bmatrix} 0 \end{bmatrix}
$$

2.3 CONTINUOUS WAVELET TRANSFORM

In the last decades, the wavelet transform has been widely used as a tool to analyze the signals. This transformation decomposes a function $f(t)$ into a superposition of the elementary function $\psi_{a,b}(t)$ derived from an analyzing wavelet $\psi(t)$ known as the mother wavelet. Wavelets are generated from the mother wavelet through scaling and translation, as defined below [18]:

$$\psi_{a,b}(t) = 2^{\frac{a}{2}}\psi(2^{a}t - b)\,, \tag{2-27}$$

where a and b are real-valued parameters, a is the scale parameter and b is the translation parameter (indicating the position). The wavelet coefficient for the time scale wavelet transform is defined as:

$$C_{a,b} = \int_{-\infty}^{\infty} f(t)\overline{\psi_{a,b}(t)}\,dt\,, \tag{2-28}$$

where $\overline{\psi_{a,b}(t)}$ is the conjugate function of $\psi_{a,b}(t)$.

Wavelet transforms are mostly employed for signal processing in the time domain. However, the objective of this research is analyzing displacement of the structure, which is a space-domain signal. By replacing the time with a spatial coordinate x in equation (2-28), spatial distributed signal $W(x)$, which is the displacement of the beam structure can be analyzed by wavelet transform over $(l1 - l2)$.

$$C_{a,b} = \int_{l1}^{l2} W(x)\overline{\psi_{a,b}(x)}\,dx\,, \tag{2-29}$$

In this study, Gabor wavelet family is used to analyze signal of the beam structure over $(0 - L)$.

This transformation is generated from Gabor function, as defined below [38]:

$$\psi(x) = \frac{1}{\sqrt[4]{\pi}}\sqrt{\frac{\omega_0}{\gamma}}\exp\left[-\frac{\left(\frac{\omega_0}{\gamma}\right)^2}{2}x^2 + i\omega_0 x\right], \tag{2-30}$$

where ω_0 and γ are calculated as 2π and $\pi\sqrt{(2/ln2)}$ in order to satisfy the admissibility condition of the Gabor wavelet family. The mean value of the mother wavelet must be zero; also, it must satisfy the admissibility condition as below,

$$\int_{l1}^{l2}|\psi^*(x)|^2\frac{d\omega}{|\omega|} < \infty\,, \tag{2-31}$$

where $\psi^*(x)$ is the Fourier transform of $\psi(x)$, derived by

$$\psi^*(x) = \int_{-\infty}^{\infty}\psi(t)e^{-i\omega t}\,dt\,. \tag{2-32}$$

By substitution of equation (2-30) to equations (2-29) and (2-27), Gabor wavelet coefficient of the spatial signal, $W(x)$, can be derived in the space domain from $l1$ to $l2$.

$$C_{a,b} = \int_{l1}^{l2} W(x)2^{\frac{a}{2}}\frac{1}{\sqrt[4]{\pi}}\sqrt{\frac{\omega_0}{\gamma}}\exp\left[-\frac{\left(\frac{\omega_0}{\gamma}\right)^2}{2}(2^a x - b)^2 + \iota\omega_0(2^a - b)\right]dx\ \ . \tag{2-33}$$

In the real applications, the displacement signal consists of a number of discrete data points. By replacing the continuous signal, $W(x)$, with discrete signal $W(x_n)$ (n=1,2…,N), equation (2-33) is transformed to equation (2-34),

$$C_{a,b} = \sum_{n=1}^{N} W(x_n)2^{\frac{a}{2}}\frac{1}{\sqrt[4]{\pi}}\sqrt{\frac{\omega_0}{\gamma}}\exp\left[-\frac{\left(\frac{\omega_0}{\gamma}\right)^2}{2}(2^a x_n - b)^2 + \iota\omega_0(2^a - b)\right].\Delta x \tag{2-34}$$

where x_n is the data points between $l1$ and $l2$, N is the number of data points, Δx is the step-size, $C_{a,b}$ is the Gabor wavelet coefficient of the discrete spatial signal $W(x_n)$ corresponding to a scale factor a and a certain position b that is between $l1$ and $l2$. A perturbation at location b of a spatial signal, will be enlarged by the corresponding wavelet coefficient value [18].

2.4 WINDOWING FUNCTIONS

Window functions are known as the mathematical functions, which are zero outside of a defined interval [39]. Many window functions have been used in the researches of different fields of study. For instance, the most used ones are Rectangular, Triangular, and Hanning functions, which are shown in Figure 2-3. Rectangular function as the simplest one is constant inside the defined interval and zero-valued elsewhere . Triangular function has the maximum value at the middle of the defined interval and it rapidly goes with a linear slope towards zero at the both ends of the interval [40]. As it is demonstrated in Figure 2-3(c), Hanning function is a discrete function given by [41]:

$$w(n) = 0.5\left(1 - \cos\left(2\pi\frac{n}{N}\right)\right) \tag{2-35}$$

where N is the number of samples.

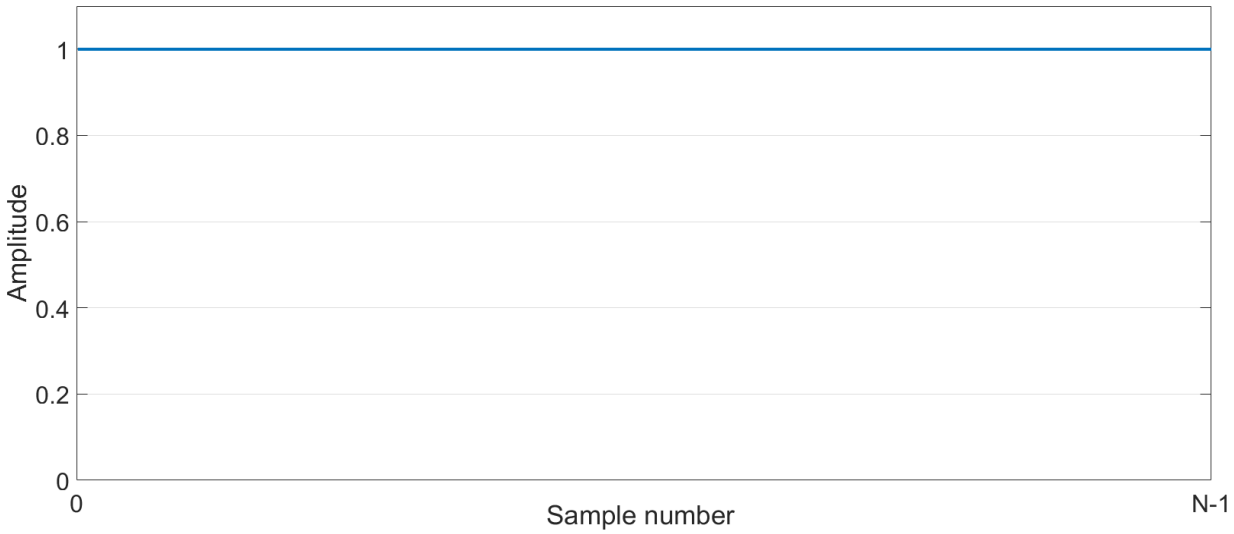
1
0.8
0.6
0.4
0.2
0
Amplitude
0
Sample number
N-1

(a)

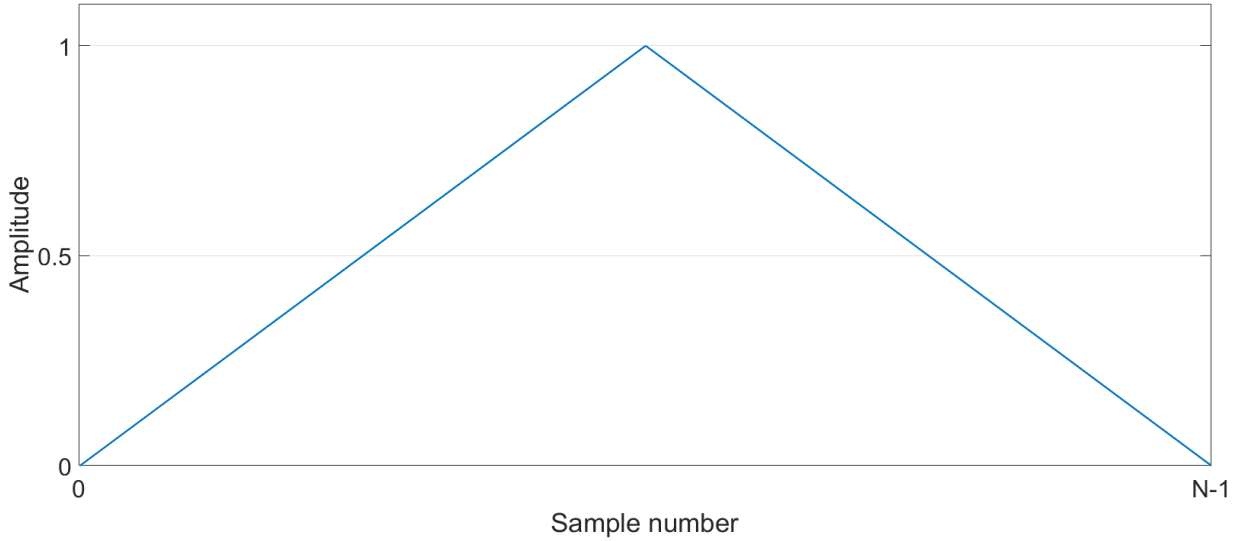
1
0.5
0
Amplitude
0
Sample number
N-1

(b)

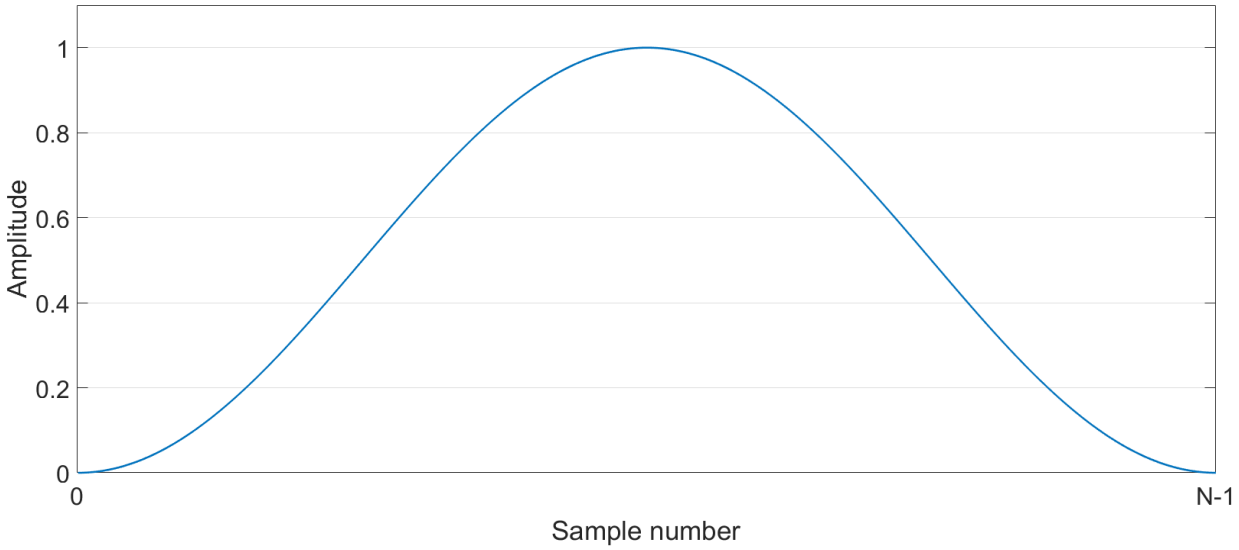

(c)

Figure 2-3 (a) Rectangular, (b) Triangular, and (c) Hanning window functions

As it has been mentioned in the introduction chapter, large coefficient values in the vicinity of the measurement boundaries are known as the edge effect in the wavelet analysis. This phenomena limits the wavelet-based damage detection, since, singularities induced by damages located close to the boundaries are covered by these large values. Window functions can be used so as to erase or reduce the edge effect in the wavelet analysis procedure. In the simulation part of the thesis, Hanning window is used and the results are presented in the chapter 3. Furthermore, Hanning, triangular, and 1-Hanning windows are applied to the signals derived from the experimental studies and results are shown in the chapter 4. Figure 2-4 illustrates 1-Hanning window function.

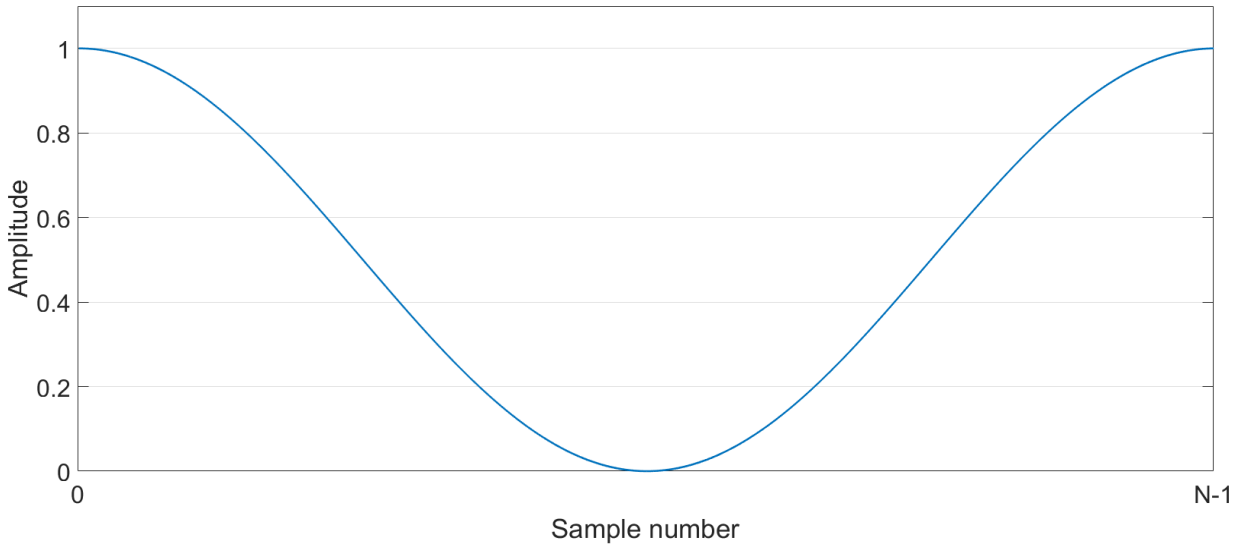

Figure 2-4 1-Hanning window function

3 SIMULATION AND NUMERICAL STUDIES

3.1 INTRODUCTION

Three mode shapes, which are derived in the previous section, are not able to show any sign of the crack existence in the beam structure. In the structural health monitoring area, wavelet transform is used to magnify small singularities or perturbations at the damage locations inside the signal of structure's behavior. In this chapter, Gabor wavelet is applied to the first three mode shapes in order to give a clear understanding of the crack detection in the structure under study. Three different parameters are found inside the wavelet analysis procedure of this study. The first parameter is the scale factor inside the wavelet transform, and the second one is the crack depth, which is representative of the crack size. The last parameter is the crack position on the beam structure. This chapter presents a parametric study on the wavelet analysis of a cracked cantilever beam. Different crack positions and depths are investigated, and then optimization procedure is conducted for choosing proper scale factor inside the wavelet transformation to achieve clear crack detection results. In the other word, the effects of crack size and position on the optimization of the scale factor are studied. Results of this simulation study are comprehensibly explained in the following section, and will be used to guide the experimental studies in the next chapter.

3.2 SIMULATION RESULTS AND DISCUSSION

The output of wavelet analysis in our study is a plot included the wavelet coefficient values along the cracked beam length. Relative wavelet coefficient is defined for sensitivity analysis by comparing the coefficient values at different positions of the beam with the lowest value in the

intact area of the beam (Wavelet coefficient is used as a short expression in the rest of the thesis). The first set of results is obtained for scale factors from 0 to 20 and is shown in Figure 3-1. At this step, crack size and position are considered as the constant values, and the wavelet coefficient values along the beam length are obtained for different scale factors. The crack depth is 12.5 percent of the beam height and it is located at the middle of the beam. Wavelet coefficients plots for all three modes reveal a large perturbation caused by the crack at its location. As it can be seen, very large wavelet coefficient values are obtained at all locations of the beam regardless of the crack position for scales greater than 8. Hence, the scales greater than 8 are not suitable choices for this study. The other point is the large coefficient values in the vicinity if the beam ends. This phenomenon is called edge effect in the wavelet analysis and refers to the nature of wavelet transform. Wavelet transform is defined for infinite number of data points, while in real applications it is employed to analyze a finite number of data points. Because of this fact, large singularities emerge near the measurement boundaries. As it is shown in the Figure 3-1, for most the scale factors edge effect is limited to small areas close to the boundaries. However, choosing some scale factors results in larger area affected by the edge effect. For instance, choosing scale factors smaller than 3 or 4 results in larger areas of edge effect. According to Figure 3-1, scales 6.5, 5.6, and 5.1 are the optimal scales for first, second and third modes, respectively. For detection of a crack during wavelet analysis procedure, two factors play important roles: first, the wavelet coefficient value at the damaged area, and second, the maximum number of wavelet coefficients, which are approximately zero in the intact area and domination of non-zero values at the crack area.

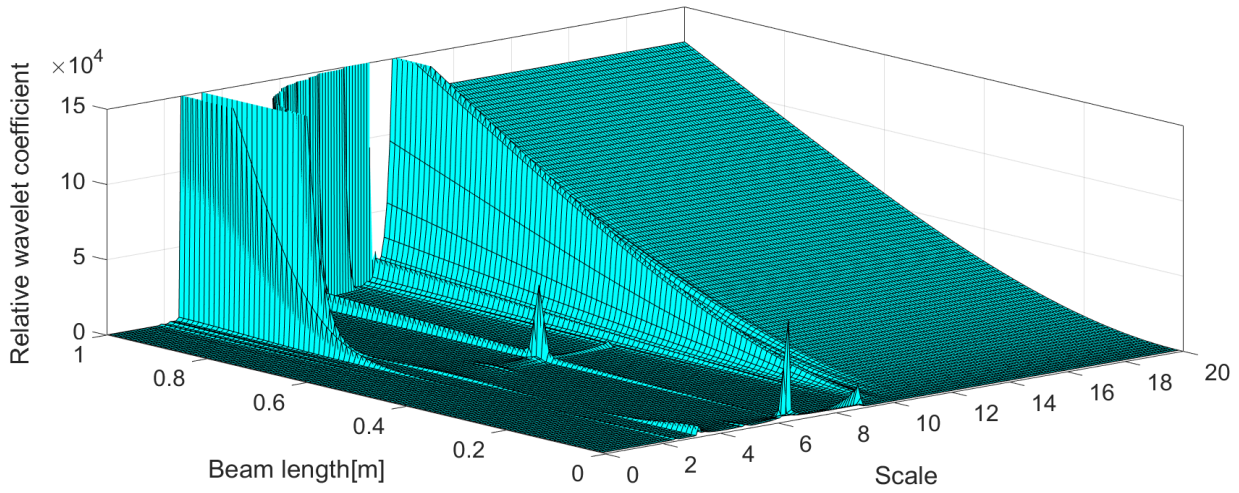
×10^4
Relative wavelet coefficient
15
10
5
0
1
0.8
0.6
0.4
0.2
0
Beam length[m]
0
2
4
6
8
10
12
14
16
18
20
Scale

(a)

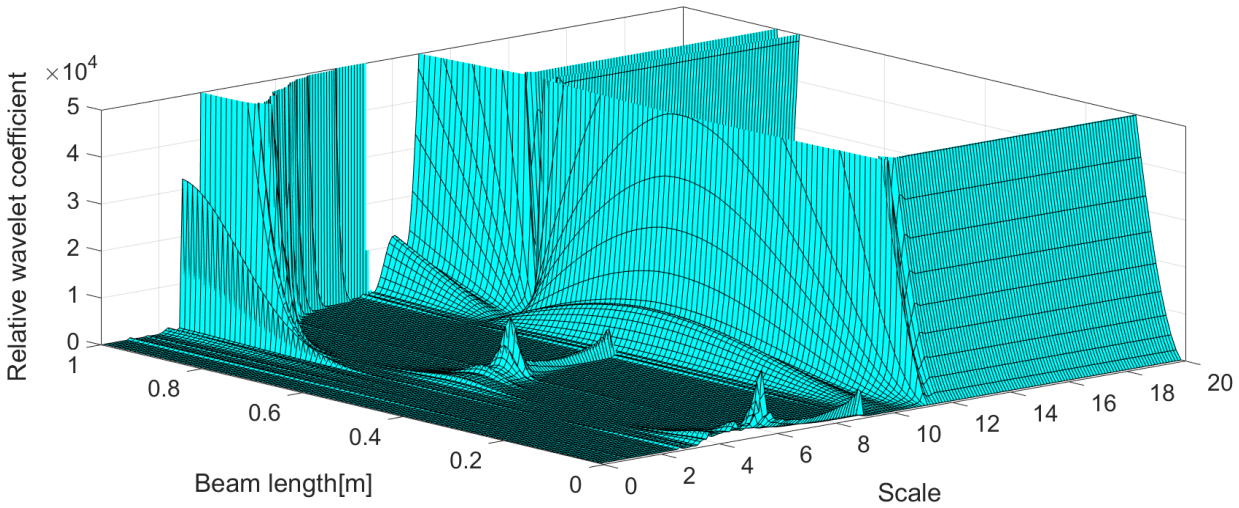
×10^4
Relative wavelet coefficient
5
4
3
2
1
0
1
0.8
0.6
0.4
0.2
0
Beam length[m]
0
2
4
6
8
10
12
14
16
18
20
Scale

(b)

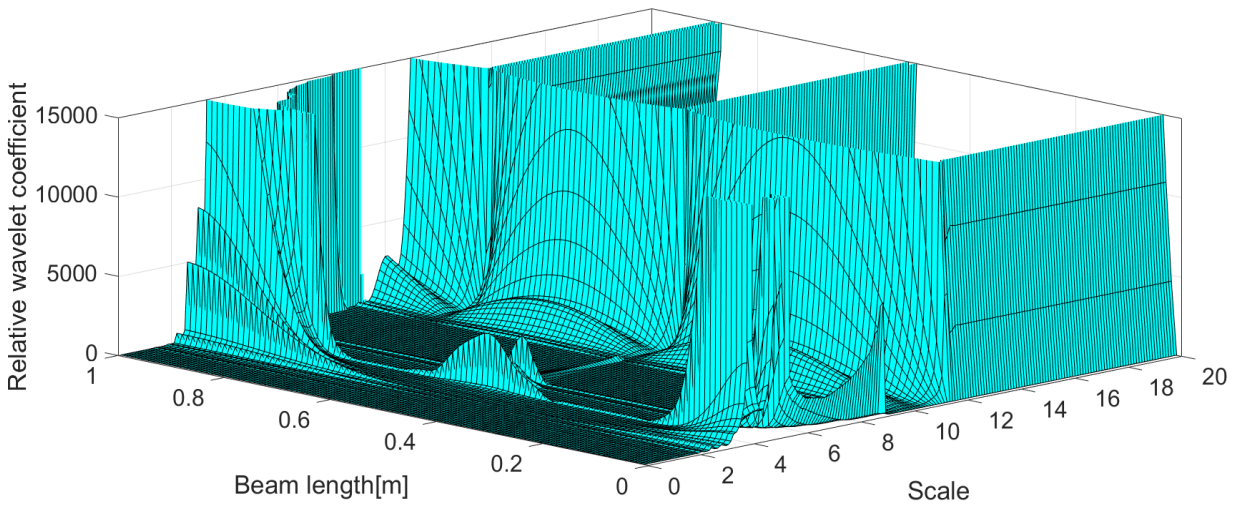

(c)

Figure 3-1 Relative Wavelet coefficients of the first three mode shapes with different scale factors at different positions of a beam with a crack at the middle (Crack depth = 0.125*Beam height). (a) First mode shape. (b) Second mode shape. (c) Third mode shape.

Figure 3-1 shows that wavelet coefficient values for the first and second modes are greater than the third mode. Wavelet coefficients are $4*10^4$, $1.5*10^4$, $3.5*10^3$ for first, second, and third mode respectively (at the crack position with optimal scales). In addition, the second mode has the maximum number of values, which are close to zero at the intact area when the optimal scale is chosen. Therefore, it can be concluded that the second mode is the most sensitive mode for identification of a crack located at the middle of the beam.

The previous discussion has clarified that the optimal scale varies for different mode shapes. Moreover, nature of the crack may also affect the results of the optimization study. The depth and the position are two important crack properties. The wavelet coefficient values at the crack location (The middle of the beam) for depths from 3 to 20 percent of the beam height are shown in Figure

3-2. Moreover, the scale factor changes from 0 to 8 so as to show the effect of crack depth on choosing the optimal scale. This figure is comprised of three 3D plots and illustrates the effect of crack depth on the chosen optimal scale for the first three mode shapes while the crack is in the middle of the beam. Although the results in Figure 3-2(a) do not include any certain rule to choose a certain optimal scale for various crack depths, 6 - 8 can be chosen as an optimal range of the scale factor. On the other hand, the derived plot based on the second mode demonstrates a certain value as the optimal scale for various crack depths, which is 5.6. For the third mode, 5.1 is the optimal scale factor. However, the wavelet coefficient values for the third mode are very small in comparison to the first and second modes. Thus, the third mode is less sensitive to detect a crack than the other two modes in this study. In this figure, comparison between the coefficient values for large and small crack depths shows this fact that the detection of large cracks is easier than the small ones as it was expected.

Figure 3-2 clearly shows the effect of crack depth on the chosen optimal scale. However, to have a complete understanding about influences of the crack nature on the chosen optimal scale, another analysis is needed. In this step, crack position as another parameter of the study varies from 0.1 to 0.9 [m] and the wavelet coefficient values at the crack position for each scale factor are obtained. Figure 3-3 illustrates the results of this analysis for the first three mode shapes.

In this part of study, the crack depth is 12.5 percent of beam height. It can be seen that the first mode is more sensitive to detect and localize cracks, which are closer to the fixed-end than the free-end of the beam. Moreover, damage detection by choosing scale factors smaller than 6 cannot be performed properly. The main findings of Figure 3-3 are the optimal scale range from 6 to 8 for the first mode, and optimal scale values 5.6 and 5.1 for the second and third modes, respectively.

Furthermore, it can be seen in Figure 3-3(b), the second mode is more sensitive to detect cracks close to the middle of the beam than the ones around the boundaries. On the other hand, the third mode is not sensitive to cracks close to the free end and middle of the beam structure. This mode has its most sensitivity to detect cracks located between the fixed end and the middle of the beam. Thus, the third mode is a more suitable choice for detection of a crack located at mentioned area and the first mode is the other choice based on the coefficient values at crack location.

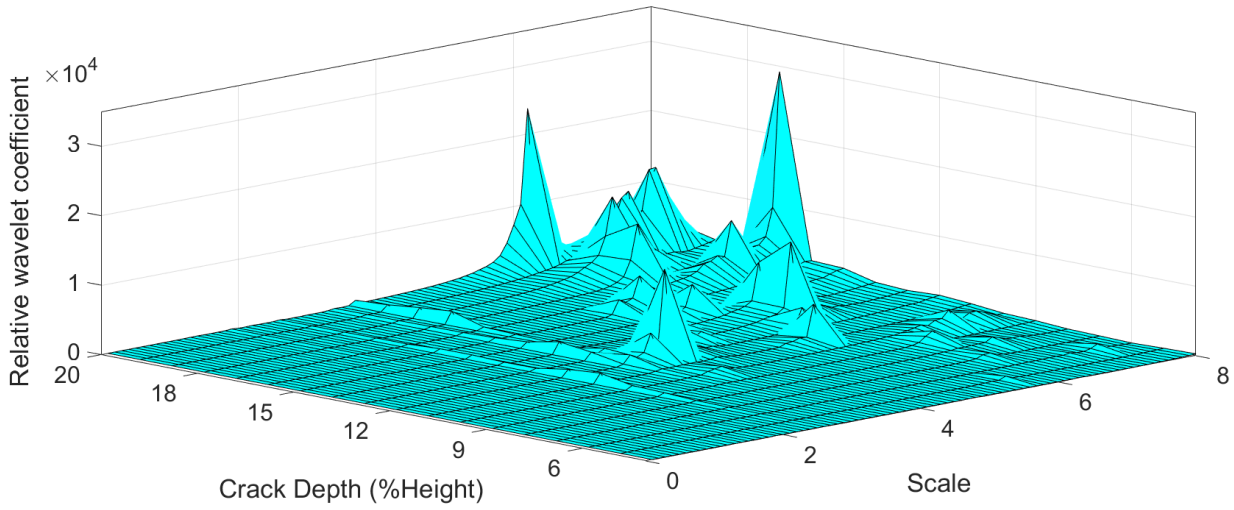

(a)

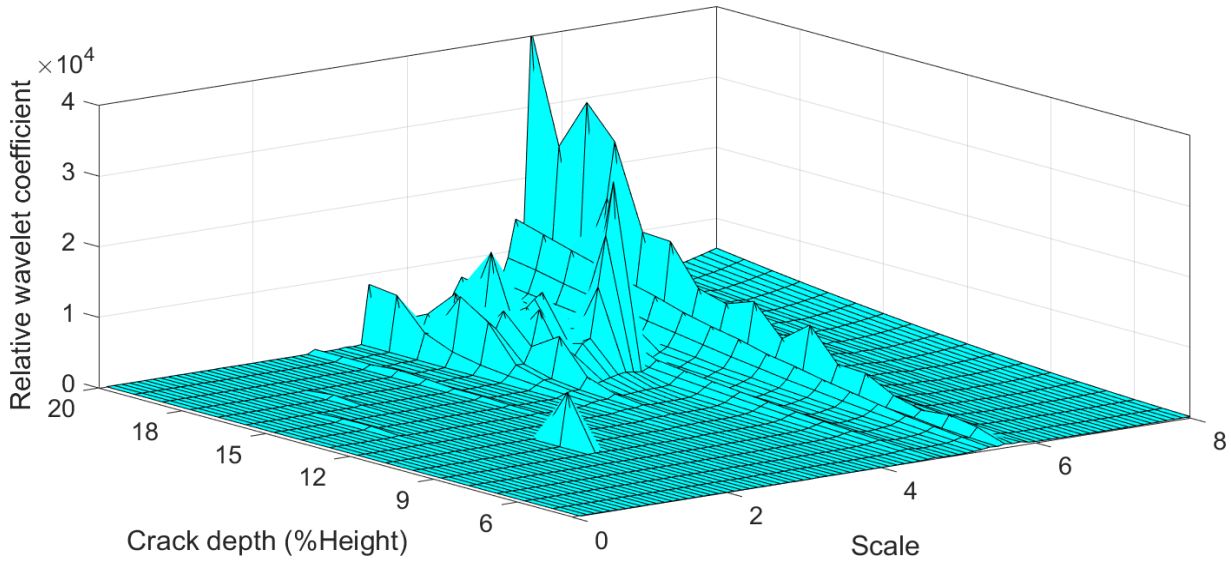

(b)

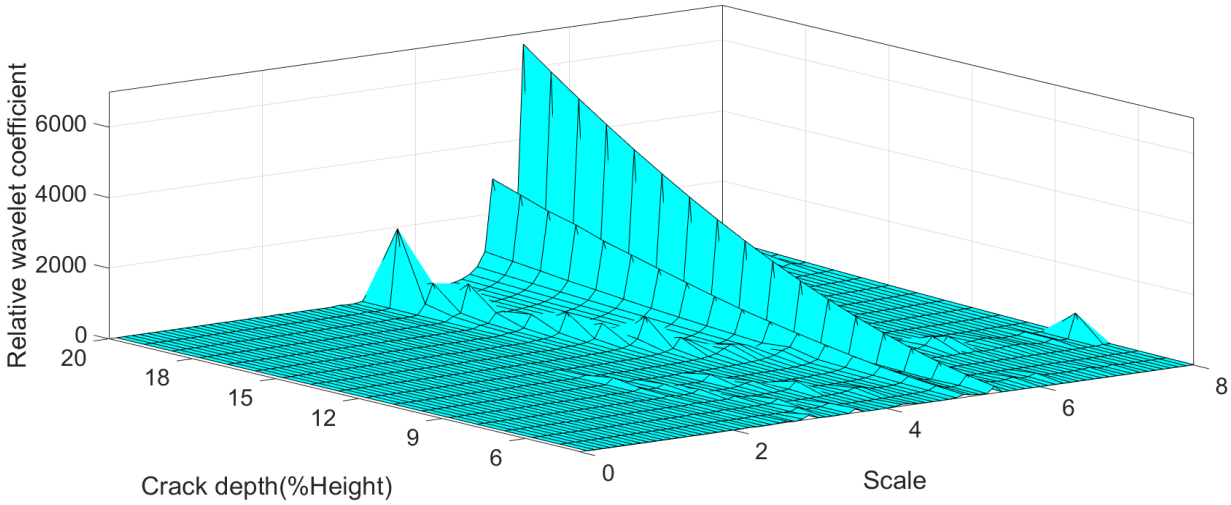

(c)

Figure 3-2 Relative Wavelet coefficient of the first three mode shapes vs. crack depth and scale with the crack at the middle of the beam. (a) First mode shape (b) Second Mode shape (c) Third mode shape

As it has been mentioned before, edge effect is considered as a significant problem of wavelet based damage detection. Those large values could make it impossible to detect cracks, which are

small or close to the boundaries. In these situations, a singularity at the crack location might be covered by the large coefficient values. Figure 3-1 illustrates that all three modes are not sensitive to detect cracks close to the fixed and free ends because of the large coefficient values around the boundaries.

The window function can be an appropriate solution to erase the edge effect around the beam boundaries. In this step of the simulation part, a Hanning window function is applied to the first three mode shapes of the cantilever beam for two different crack locations. In one case, a crack is located at a position of 0.1 m, which is close to the fixed end and in the other case, crack is located at 0.9 m. The crack depth in both cases is 12.5 percent of the beam height. Afterward, the Gabor wavelet transform is applied to the windowed mode shapes and results for a crack located close to the fixed end are presented in Figure 3-4. Same as the previous obtained results, large wavelet coefficient values at the crack position prove that the first mode has the most sensitivity to detect and localize a crack close to the fixed end of the beam. This figure indicates an obvious perturbation at the crack position. However, except an intense peak at the damaged spot, a smooth perturbation appears in the middle of the beam. This smooth perturbation is due to the nature of the Hanning window function and can be seen in all three modes. As another finding from this figure, the edge effect is erased in areas close to the boundaries. Moreover, the optimal wavelet scale for all three modes is found around 8. Figure 3-5 shows the wavelet coefficients plots for a beam with a crack located at 0.9 m of the beam length. As it can be observed, the first mode does not show a clear sign of the crack existence. However, the other two modes are able to demonstrate the crack effect in the signal by a significant singularity at the crack location. The coefficient values at the crack location show the fact that the third mode is more appropriate than the second one to

detect a crack close to the free end of the beam structure. The smooth perturbation caused by the Hanning window could lead to a concern regarding the detection of cracks located at the middle of the beam structure. Figure 3-6 clarifies that even in such cases a crack can be identified by a significant singularity at the crack location. In this case, the second mode gives the best result for the crack detection. Eventually, it can be concluded that by using proper window function, wavelet-based damage detection method is applicable even for small cracks close to the both ends.

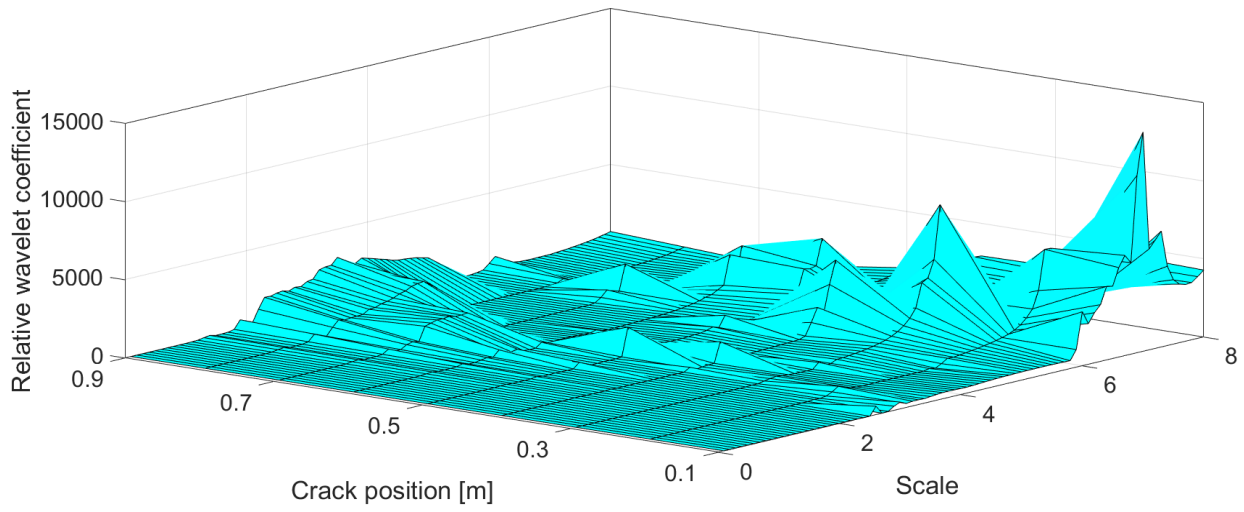

(a)

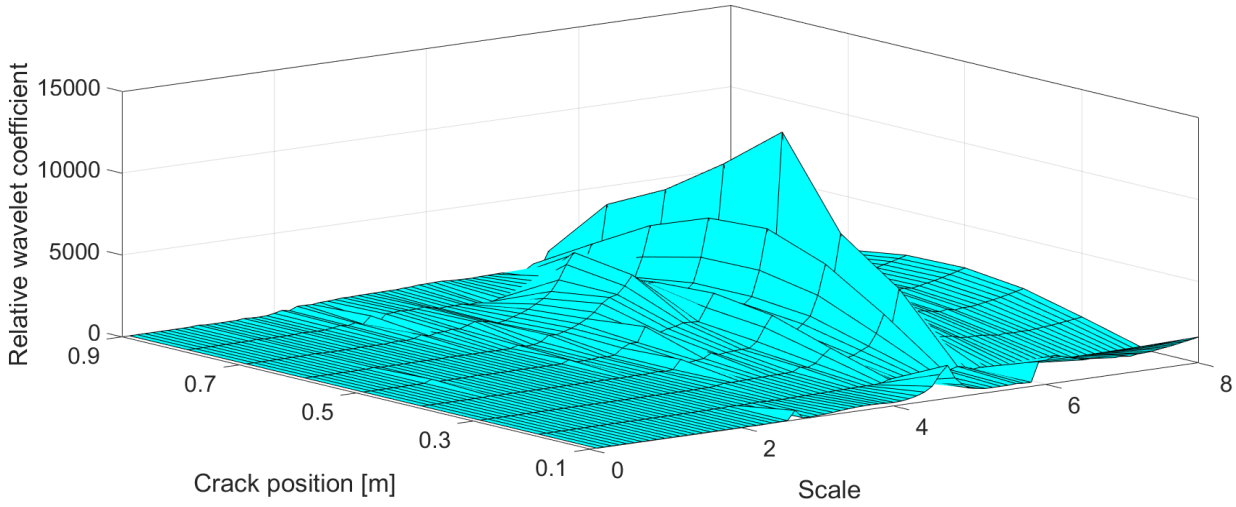

(b)

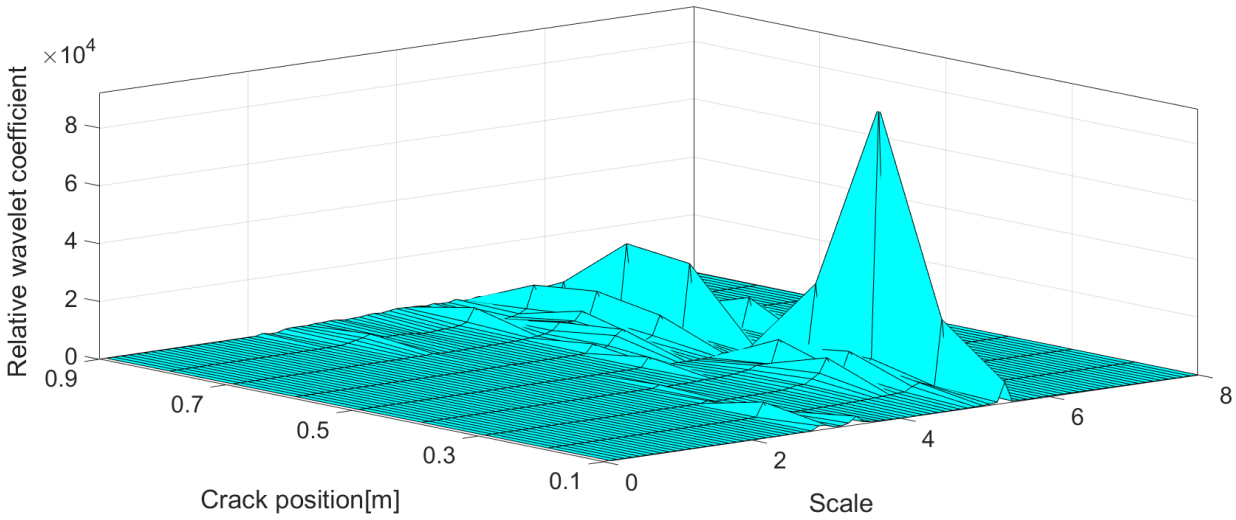

(c)

Figure 3-3 Relative wavelet coefficients of first three mode shapes of a beam with a crack at 9 different positions for various scale factors. (a) First mode shape (b) Second Mode shape (c) Third mode shape

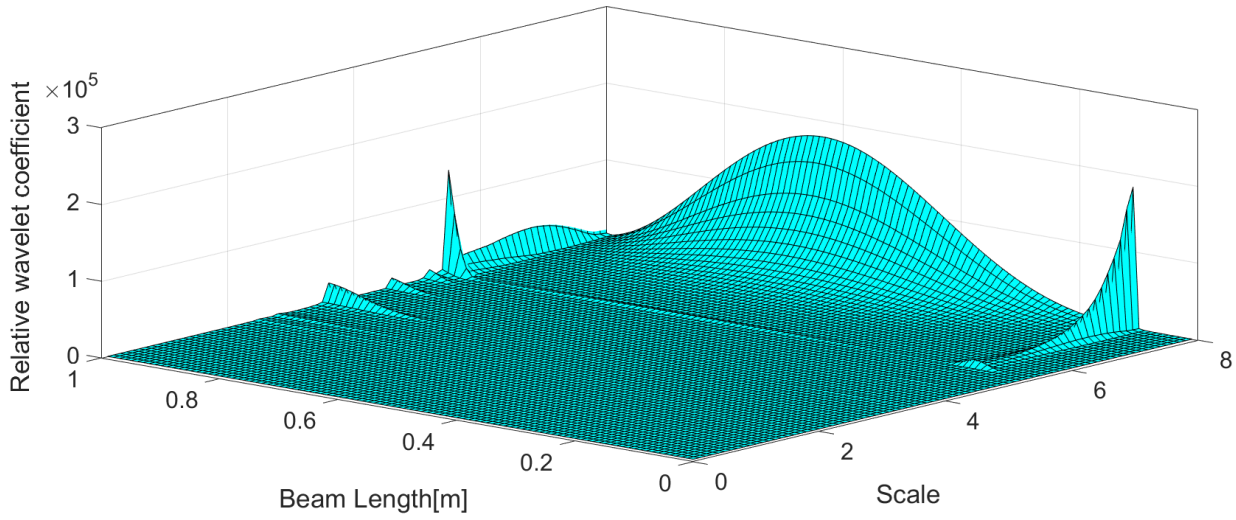
×10^5
Relative wavelet coefficient
3
2
1
0
1
0.8
0.6
0.4
0.2
0
Beam Length[m]
0
2
4
6
8
Scale

(a)

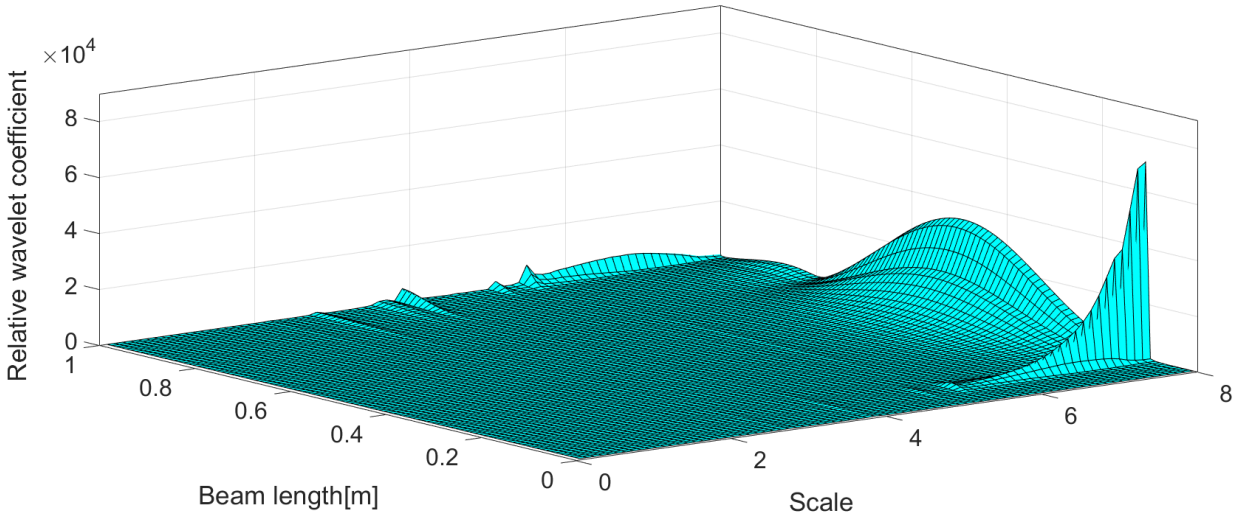
×10^4
Relative wavelet coefficient
8
6
4
2
0
1
0.8
0.6
0.4
0.2
0
Beam length[m]
0
2
4
6
8
Scale

(b)

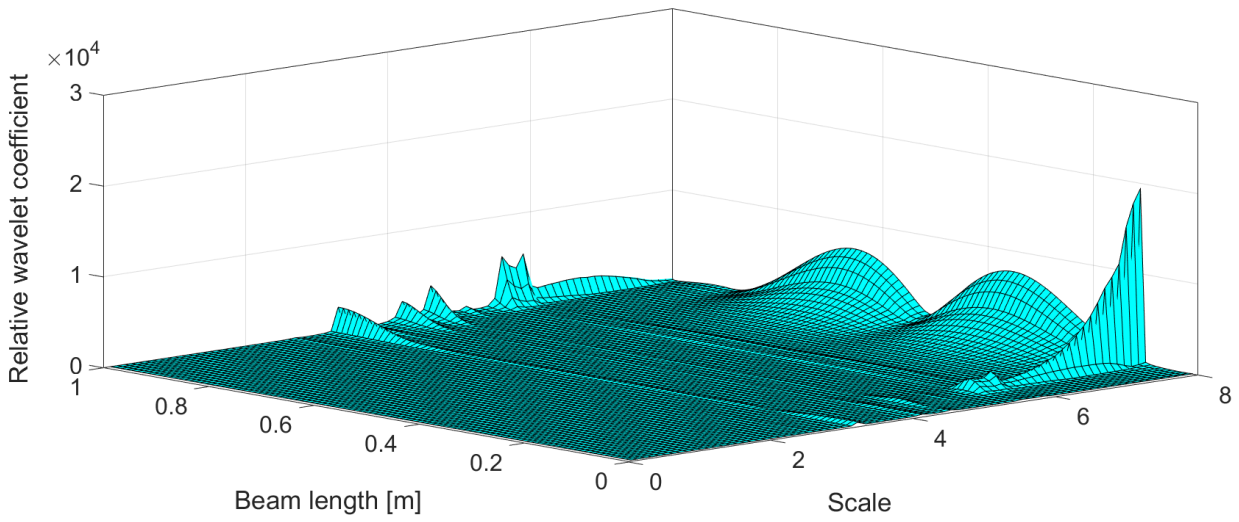

(c)

Figure 3-4 Relative Wavelet coefficient of the first three windowed mode shapes with different scale factors at different positions of a beam with a crack close to the fixed end (Crack depth = 0.125*Beam height). (a) First mode shape (b) Second Mode shape (c) Third mode shape

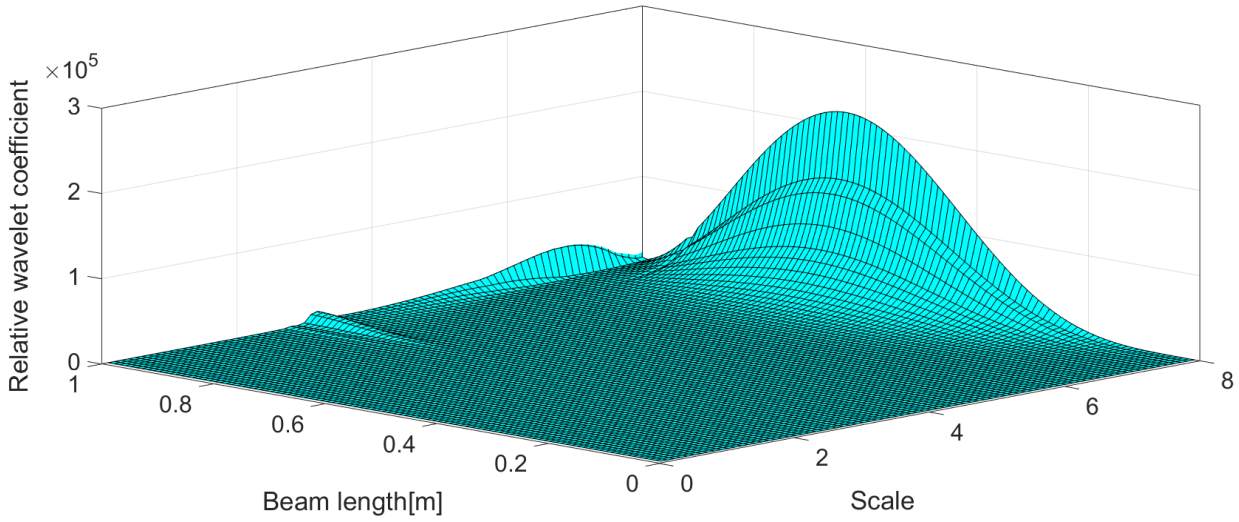

(a)

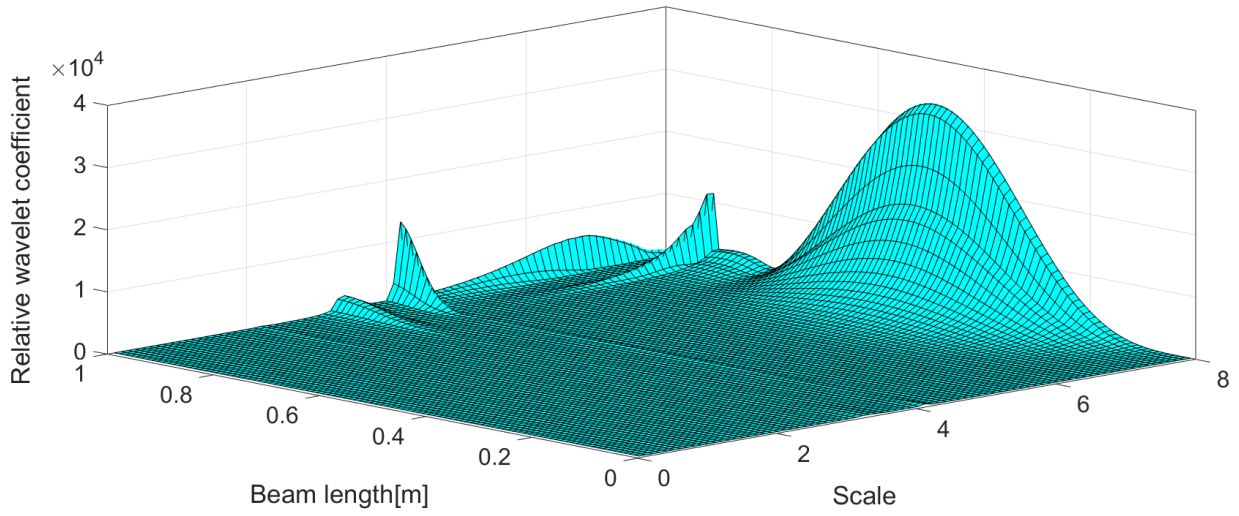

(b)

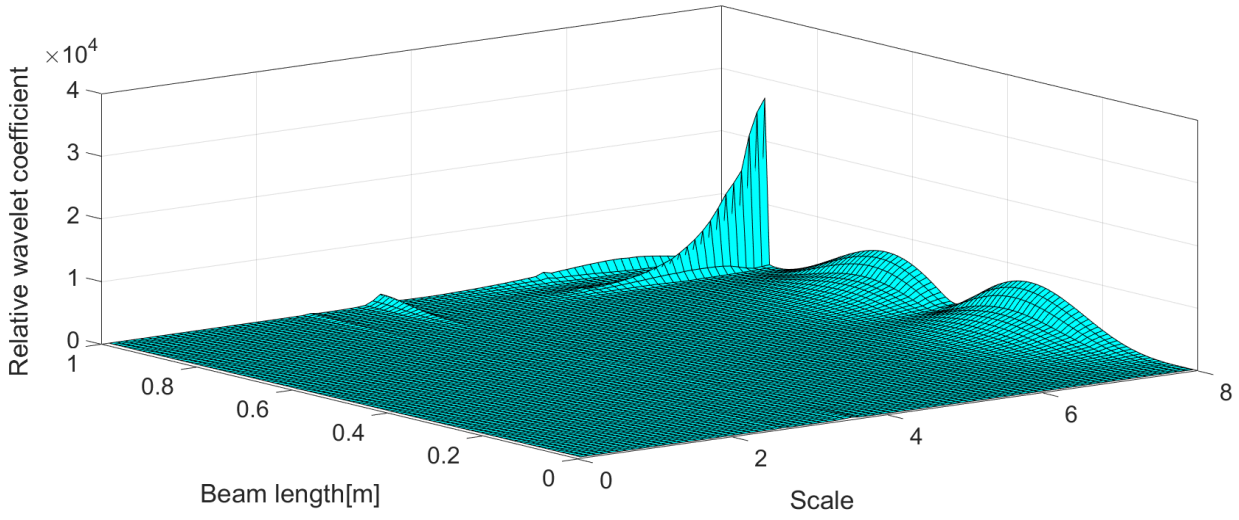

(c)

Figure 3-5 Relative Wavelet coefficient of the first three windowed mode shapes with different scale factors at different positions of a beam with a crack close to the free end (Crack depth = 0.125*Beam height). (a) First mode shape (b) Second Mode shape (c) Third mode shape

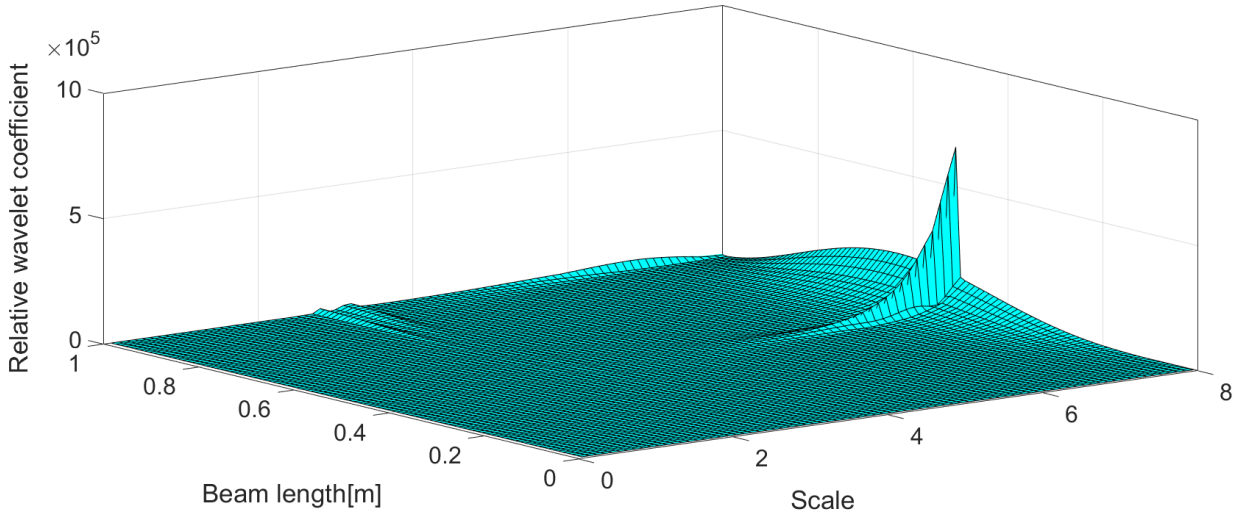
×10^5
Relative wavelet coefficient
10
5
0
1
0.8
0.6
0.4
0.2
0
Beam length[m]
0
2
4
6
8
Scale

(a)

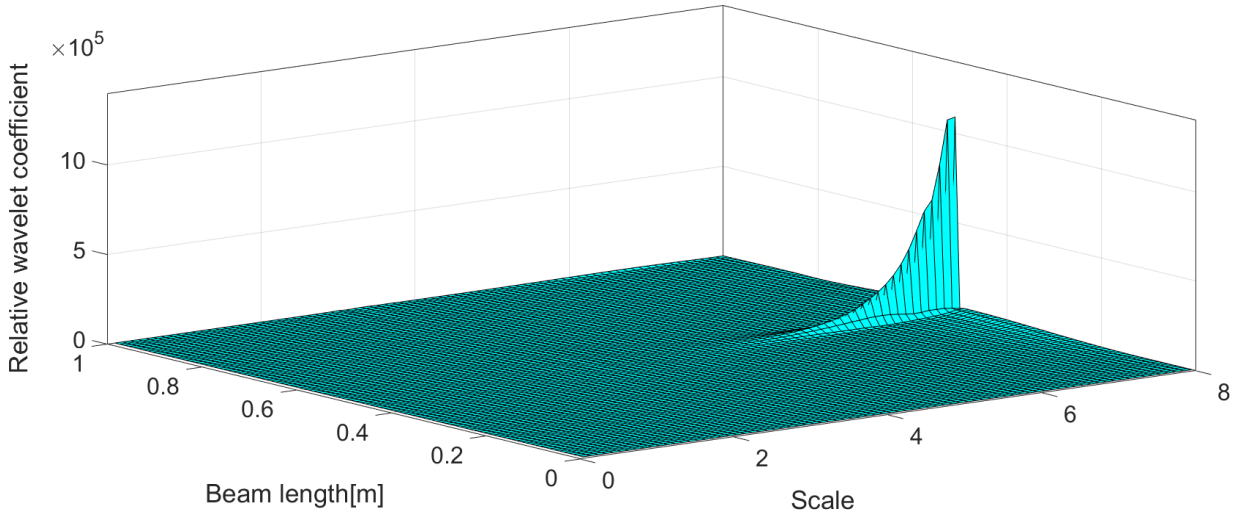
×10^5
Relative wavelet coefficient
10
5
0
1
0.8
0.6
0.4
0.2
0
Beam length[m]
0
2
4
6
8
Scale

(b)

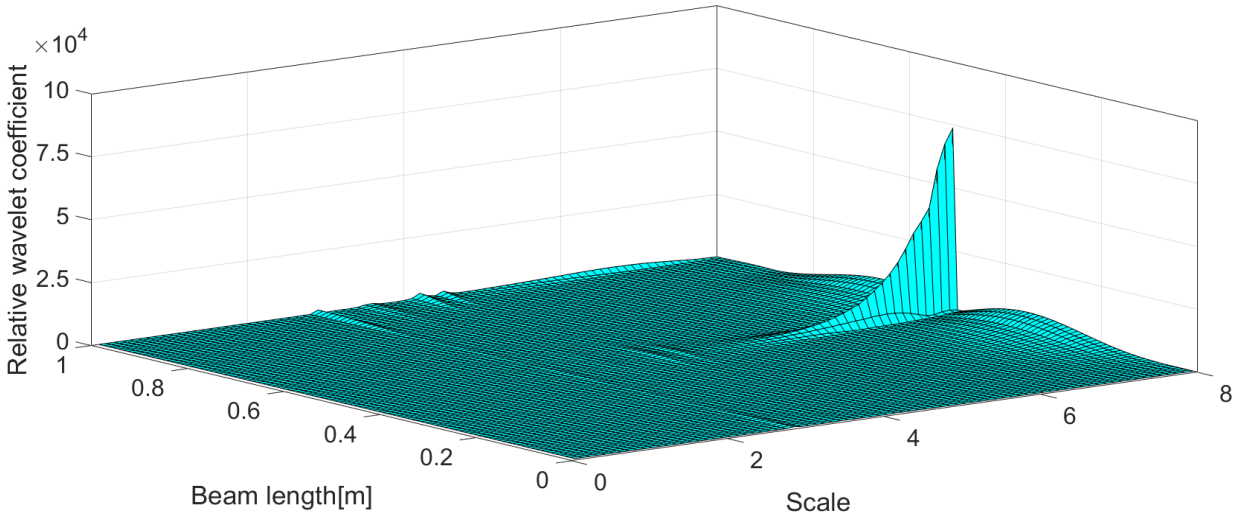

(c)

Figure 3-6 Relative Wavelet coefficient of the first three windowed mode shapes with different scale factors at different positions of a beam with a crack at the middle (Crack depth = 0.125*Beam height). (a) First mode shape (b) Second Mode shape (c) Third mode shape

4 EXPERIMENTAL STUDIES

4.1 INTRODUCTION

In all engineering research, three steps should be carried out so as to achieve real and reliable results. First of all, theoretical background and model are needed to create the initial image of the problem and its solution. As the next step, simulation studies based on the theoretical model lead to a beginning conclusion regarding the functionality of the proposed solution. Finally, experimental studies can validate the simulation results and lead to reliable and clear conclusions.

In this chapter, experimental studies are conducted to verify the results of simulation part. In the following sections, experimental set up and results are clearly presented.

4.2 EXPERIMENT SET-UP

Figure 4-1 and Figure 4-2 show the experimental set up, the aluminum beam, and a high resolution laser profile sensor (CrossCheck laser profile sensor model CC3100-30). The set up base is made of wood and one end of the beam is fixed with two screws while the free end is subjected to 15 cm displacement. The deflection slope of the beam keeps increasing along the length direction getting away from its fixed end. Table 4-1 gives the aluminum beam dimensions. As it is shown in Figure 4-3, a V-shaped crack is made on the lower surface of the beam structure and an Optical microscope (Nikon SMZ800) takes the top and front views of the crack. This figure shows the depth (0.033 cm), and the width (0.048 cm) of a crack located at a position of 35 cm from the fixed end of the cantilever beam. According to the beam dimensions in Table 4-1, the crack depth is equal to 10% of the beam height. In this study, the laser covers around 2-3 cm of the beam length

(opposite side of the cracked surface), and this covered length depends on the distance between the laser and aluminum beam surface. Although the crack is located inside the laser-covered area in order to be identified, its exact location in the detection range is unknown for the localization purpose of the study.

This study may encounter with some sources of errors and noises such as light beams from the environment, and surface roughness. The beam surface is polished by sand paper (Grade 2500) to reduce noises induced by surface roughness. Figure 4-4 demonstrates the polishing effects on the surface. In addition, the main data set in the experimental study is obtained by subtracting data sets of intact and cracked deflected beam under the same loading and working condition. This subtraction leads to have a data set with the minimum noise effect from the surface condition. In the practical operation, all measured space domain data during the monitoring should be compared with the healthy stage data to detect the possible damage. In this case, the only difference between the intact and cracked data sets is the existence of the crack. Figure 4-5 shows both sets before subtraction. It should be mentioned that each set is obtained by averaging 10 sets of data at the same measurement location of the beam. The final step to reduce the noise of the obtained signal is using smooth function in MATLAB, which smooths the data using a moving average filter.

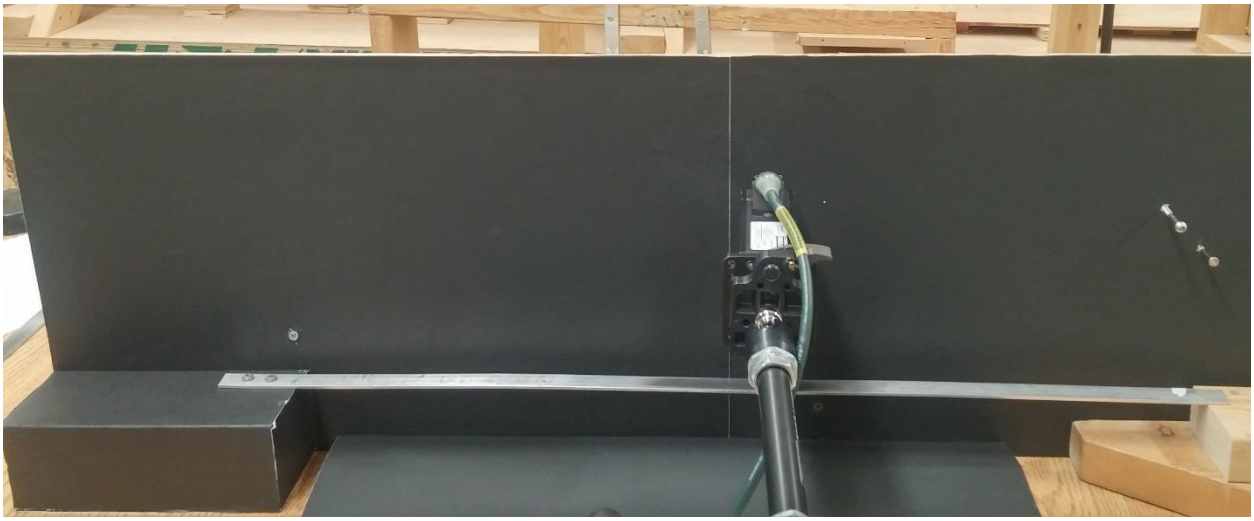

(a)

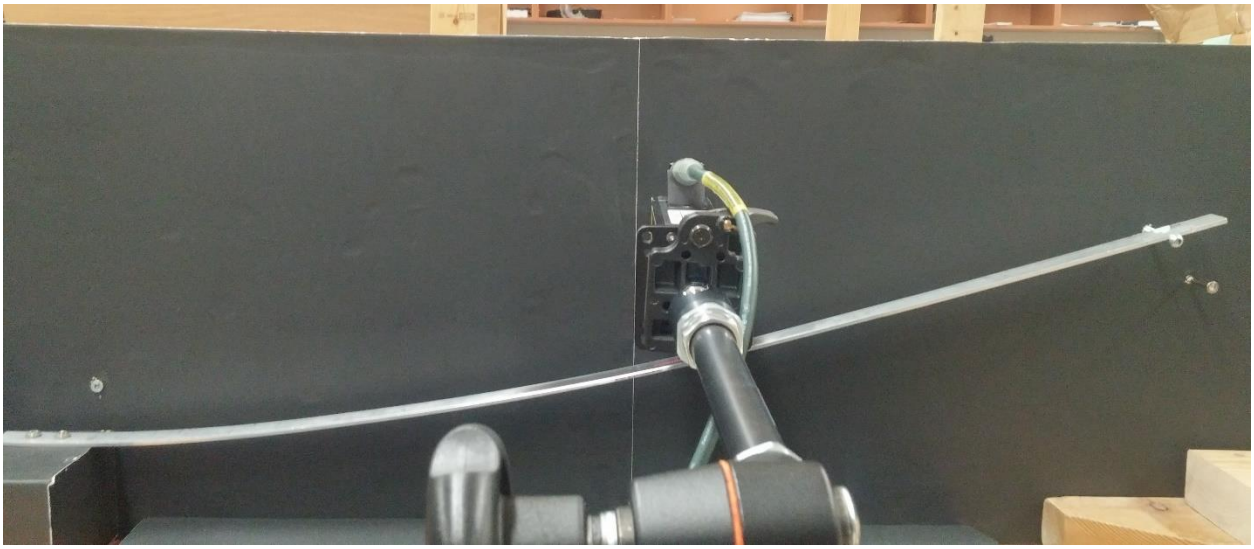

(b)

Figure 4-1 Experiment set up (a) Non-deflected, (b) Deflected

Figure 4-2 Laser beams shot on the tested beam surface

Table 4-1 Aluminum beam dimensions

Description	Quantity
Length	750 mm
Height	3.3 mm
Width	20 mm

4.3 EXPERIMENTAL RESULTS AND DISCUSSIONS

Displacement plots in the Figure 4-5 are not able to reveal the effect of the crack on the data. Gabor wavelet transform is employed as a signal-processing tool to analyze the data and magnify the crack effect. To start the wavelet analysis procedure, subtracted data set is used as the input of

wavelet transformation. This data set is obtained from 2.65 cm of the beam length, which includes 1080 points. The obtained results after applying wavelet transform to the data set one time are not capable of showing a clear outcome for crack localization. Choosing the scale factor of Gabor wavelet transform is based on the obtained range from the simulation study. The Scale factor range of 6 - 8 is considered as an optimal range when the deflection curve is similar to the first mode and data point number is around 1000. Thus, scale factor of wavelet transformation is being altered from 6 to 8 by step length of 0.1. Although the wavelet transformation with different scale factor (6-8) is being applied, wavelet coefficients after applying the transform for one time, show a noisy result which is not reliable for crack localization. Consequently, the optimization procedure for scale factor and repetition number (the number that wavelet is applied to the signal) is conducted to reach the best result. After applying wavelet transformation multiple times with different repetition number and scale factor in the optimized range, the results show an obvious enhancement for crack localization. Figure 4-6 shows some of the results of five different scale factors with wavelet repetition number 3, 4, and 5. By comparing the results, it can be seen that a clear peak perturbation appears near the middle of the signal for the optimized repetition numbers and scale factors. Increasing the repetition number to 4 with scale factor of 7.5 causes a significant large singularity at the location, where same peak perturbations appeared for different repetition numbers. Existence of this perturbation giving us the confidence of the localization of the crack with optimized wavelet scale. For repetition numbers larger than 5, the amplification rate of noises increases and the result includes many perturbations. Thus, optimization of scale factor and repetition number of wavelet transformation results in choosing scale 7.5 and repetition number 4 as the optimal values for this set of data. As it can be seen in the Figure 4-7, results of wavelet repetition number 4 with scale factor of 7.5 illustrate a clear perturbation as the indicator of a crack

at position of 13.8 mm in the spatial signal. To prove that the appeared singularity is induced by the crack, the scanning range of the laser is moved 2.5 mm to the free end of the beam. Consequently, the results with the optimized repetition number and the scale factor demonstrate that the singularity in the previous results moved 2.5 mm to the left (Figure 4-7). Existence of similar large perturbations at different locations after moving the scanning range leads to a conclusion that this perturbation appears due to the crack existence in the structure.

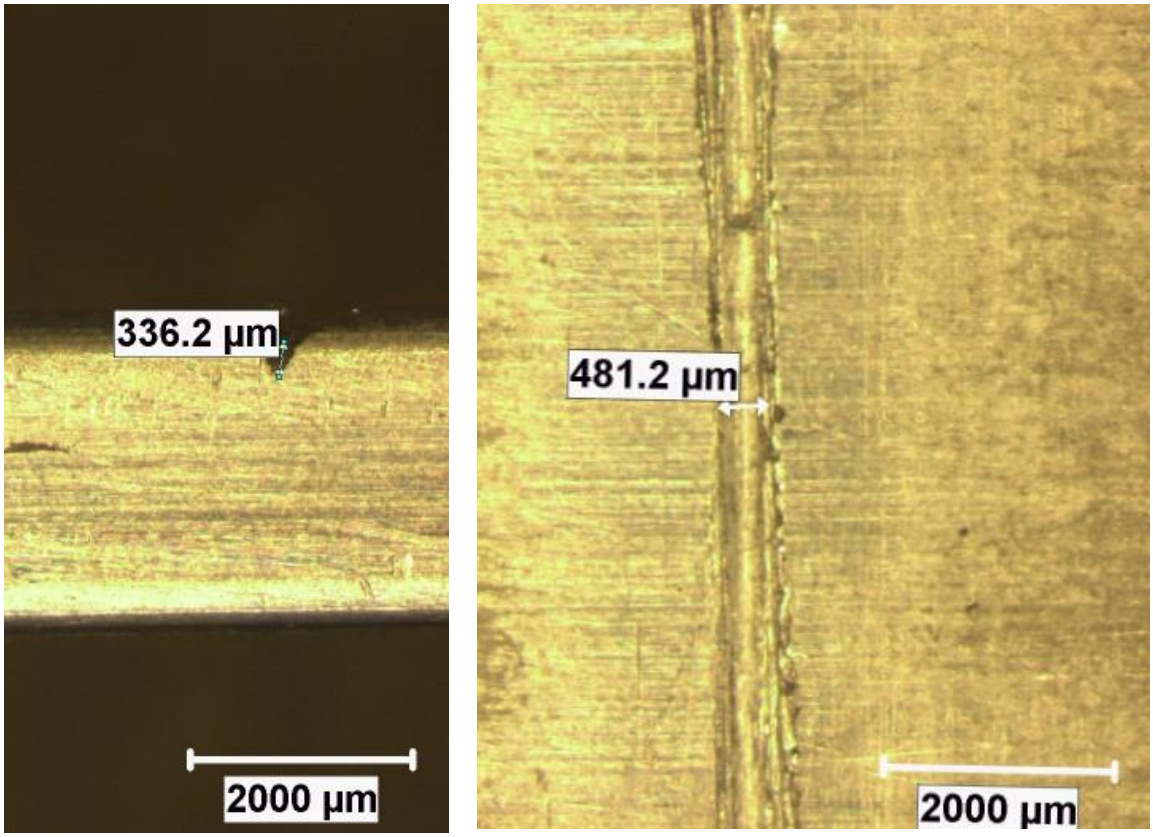

(a) (b)

Figure 4-3 (a) Side view of the crack, (b) Top view of the crack on the beam surface, (The thickness of the aluminum alloy beam is 3.3mm)-Taken by optical microscope (Nikon SMZ800)

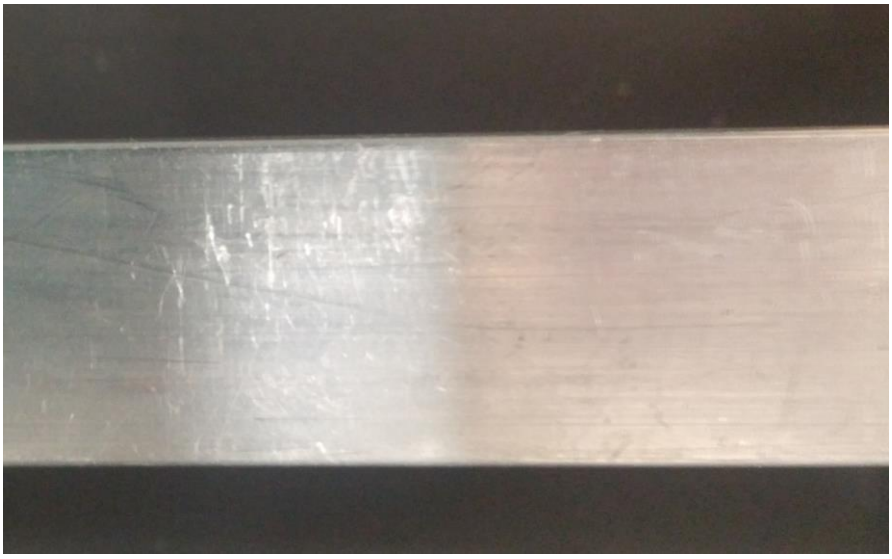

(a)

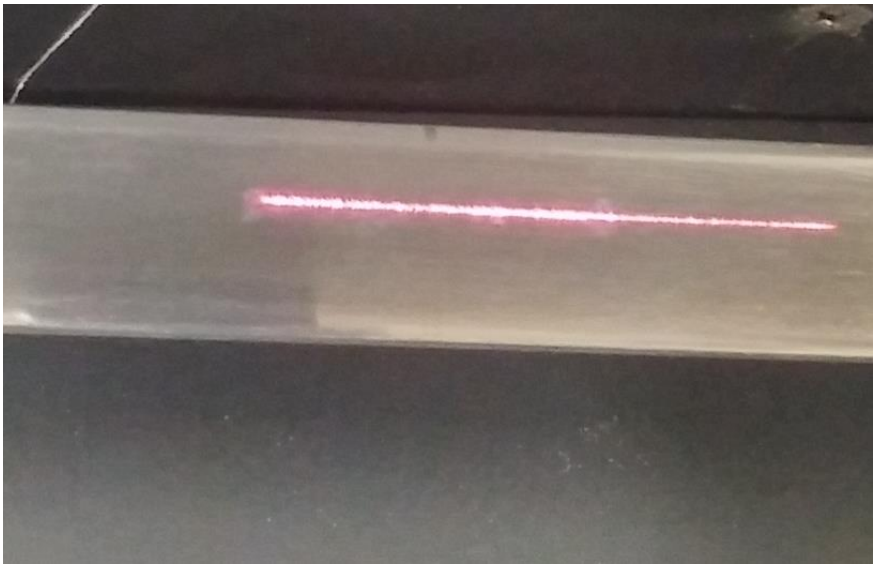

(b)

Figure 4-4 The beam surface: (a) Before polishing, (b) After polishing

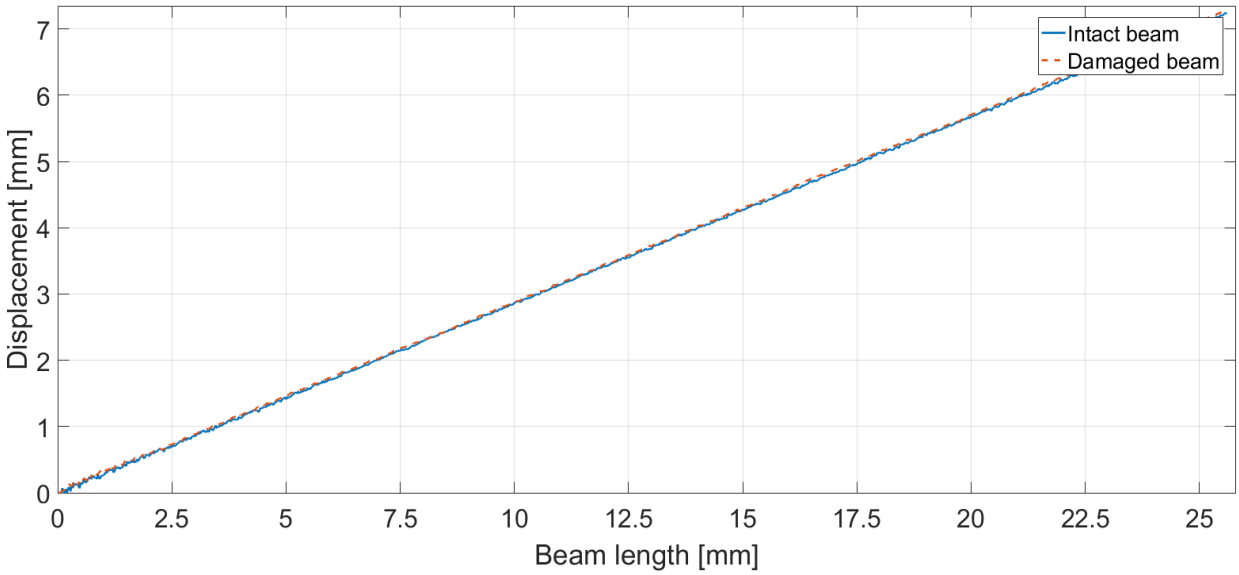

Figure 4-5 Displacement plots of the damaged beam: cracked (Orange, dotted) – Non-cracked (Blue, solid).

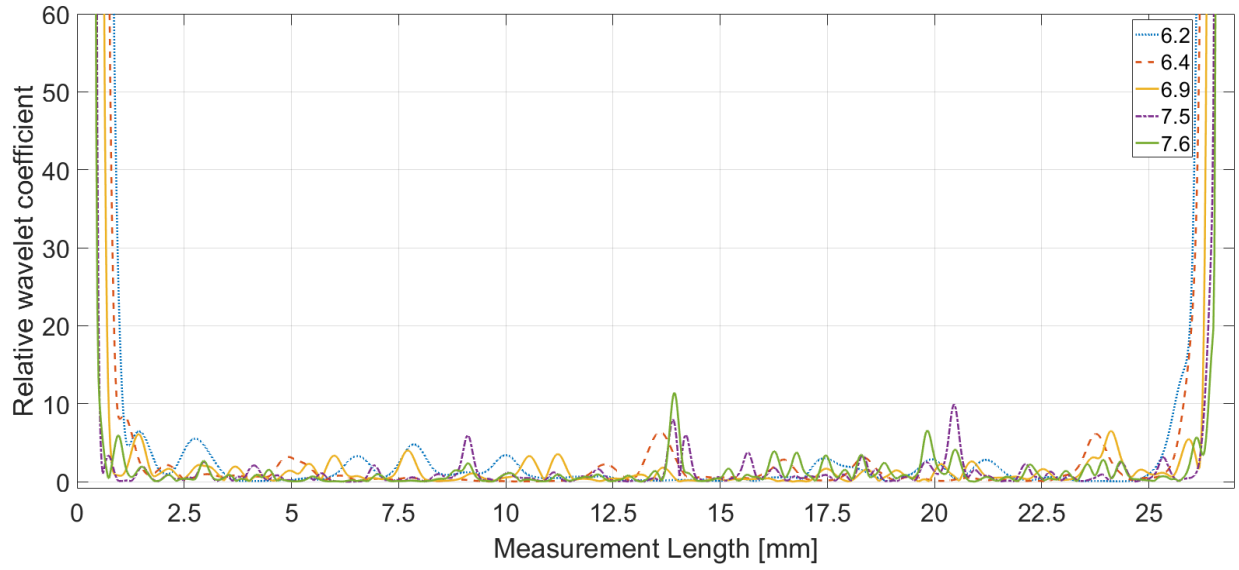

(a)

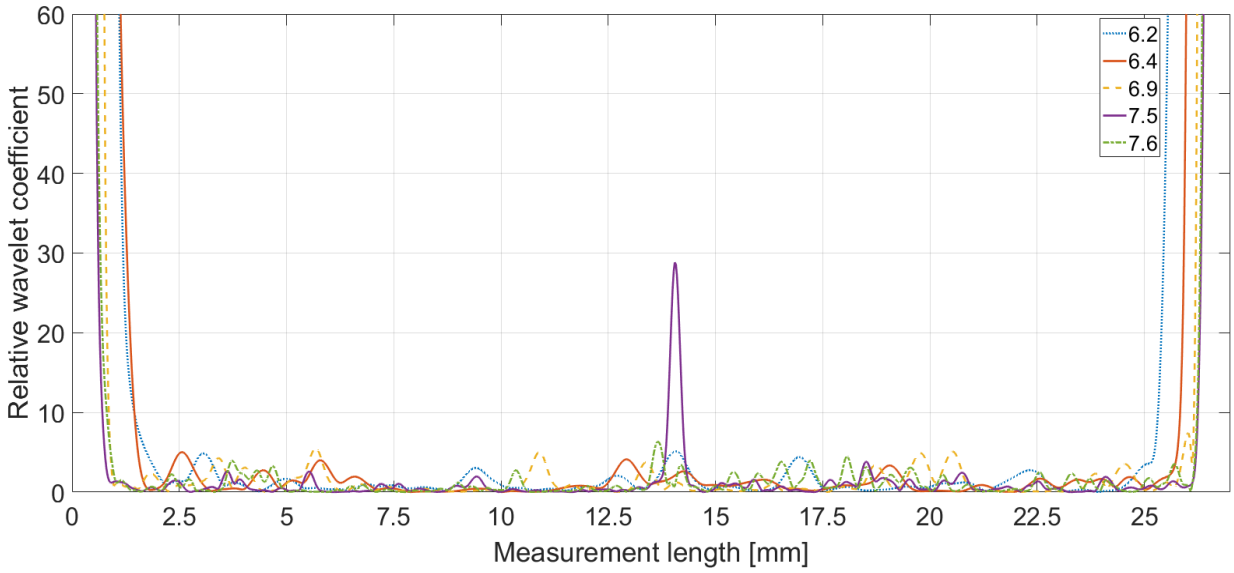

(b)

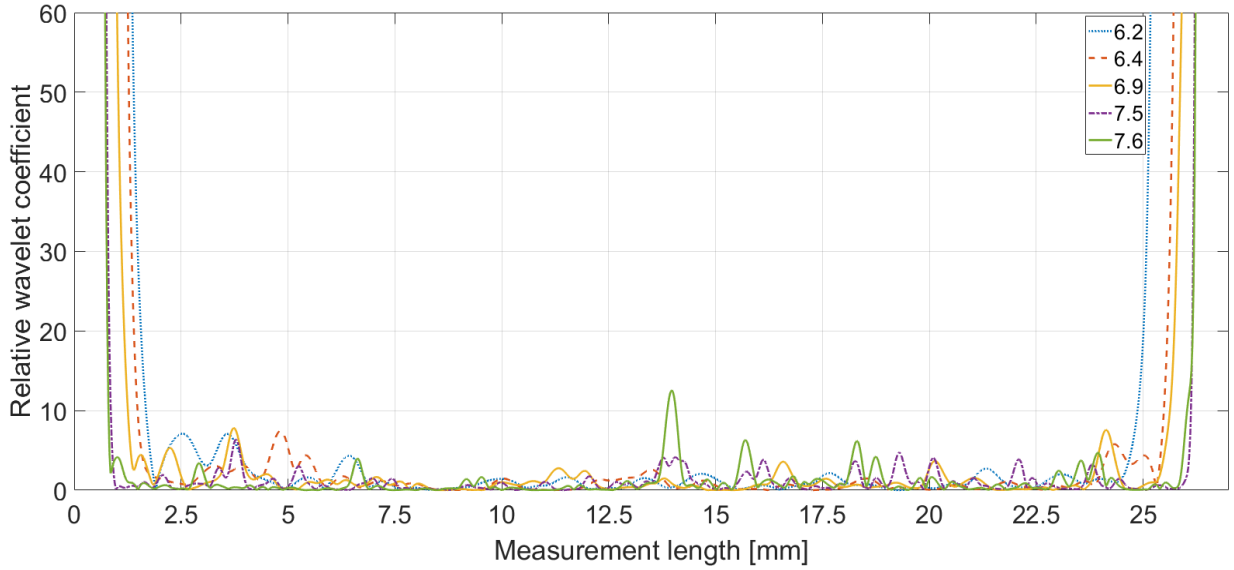

(c)

Figure 4-6 Wavelet transformation optimization process for relative wavelet coefficients of the subtracted data along the measurement length for five different scale factor with repetition numbers: (a) 3, (b) 4, (c) 5.

A new test is also performed on a different beam with same dimensions (Table 4-1) and same crack sizes as previous one (Figure 4-3). The crack is located at a position of 30 cm from the fixed end of the cantilever beam. The experiment on a new beam results in having different number of data points from the measurement signal compared with the previous case. Some reasons such as environmental lights, surface roughness, or changes in the laser position compared to the first case lead to a different covered area by the laser. In this case, the laser covers 2.15 cm of beam length, which includes 880 data points around the crack location. The number of data points directly related to the optimization which results in different optimal scale and repetition number in the wavelet analysis procedure. For this new cracked beam, the same optimization procedure as the previous case is conducted then scale factor 7.4 and repetition number 9 are obtained as the optimal values in this case (Figure 4-8). In Figure 4-8, a singularity caused by the crack emerges at position 0.61 cm of the measurement range. It is noticed that for different beams, working conditions and measurement ranges, the optimized wavelet transformation providing good crack localization could be different. In practical operation, the scale and repetition number optimization progress should hence be conducted in order to find the optimized wavelet transformation and lead to the confident localization results. This optimization procedure is highly efficient and only takes around 120 seconds to show the optimized results on a computer with 3.6 GHz CPU speed and 8GB RAM.

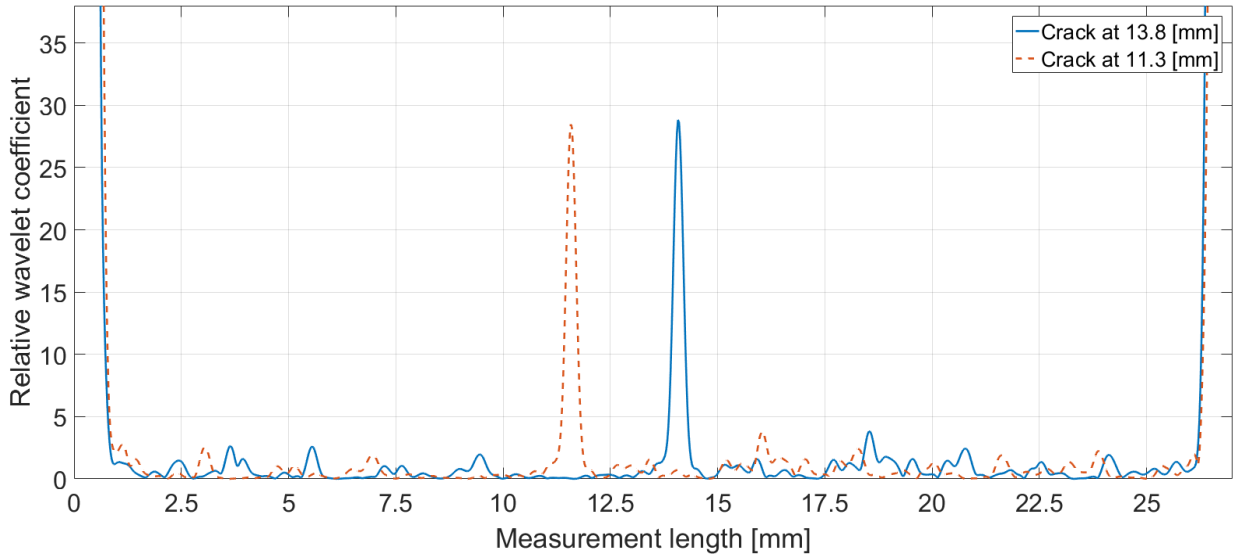

Figure 4-7 Relative wavelet coefficients of the subtracted data along the measurement length after applying optimized wavelet transform for 4 times (Scale factor =7.5, Crack positions: Blue =13.8mm, Orange=11.3 mm)

As mentioned in previous sections, during the wavelet analysis, edge effect is defined as the large values of wavelet coefficient around the measurement boundaries. Large wavelet coefficient values cover perturbations induced by cracks close to the boundaries, thus, wavelet-based damage detection methods face with problems during the detection of these cracks. Optimization for the second beam gives the optimized repetition number and scale factor for the mentioned data set. In this case, crack location is found and then by changing the measurement range of the laser sensor on the second beam sample, crack location gets close to the measurement boundary. The scanning range of sensor moved 5.25 mm to the right side then the new crack location is 0.85 mm from the left end of measurement boundary. The wavelet coefficient results with the crack located close to the measurement boundary are also given in Figure 4-8. It can be seen that in this figure, there is no visible singularity caused by the crack at a location of 0.85mm. In other words, in Figure 4-8,

large coefficient values close to the left end cover the singularity induced by the crack closed to the measurement edge.

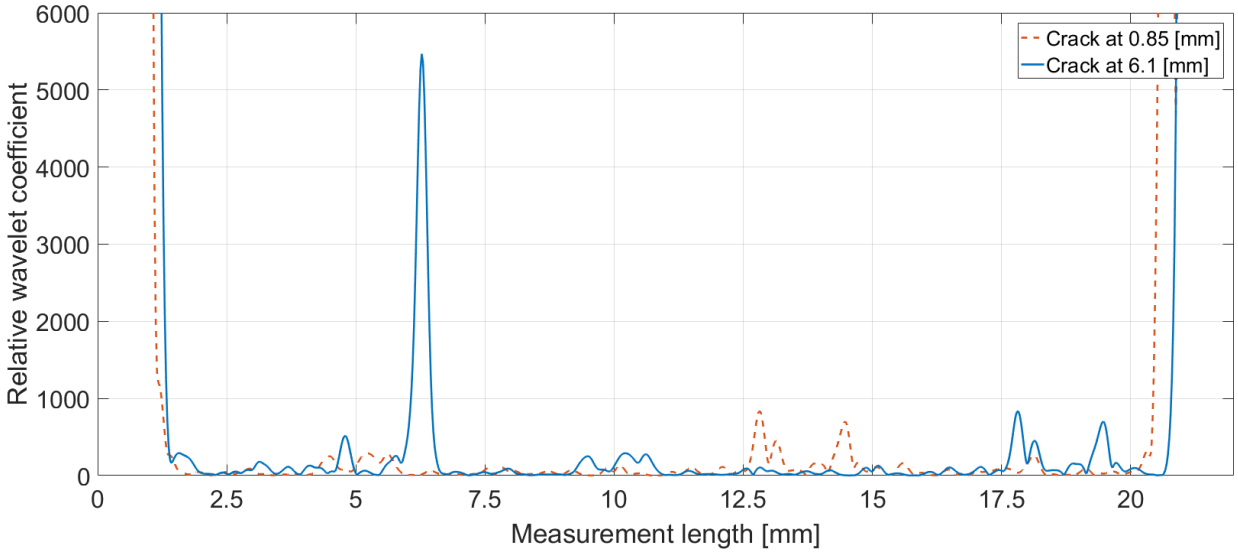

Figure 4-8 Relative wavelet coefficients along the measurement length of the second beam sample (Repetition number = 9, Scale factor = 7.4, Crack positions: Blue=6.1mm, Orange=0.85mm)

Window functions are hence introduced as a solution to reduce or erase the edge effect of the wavelet analysis in this study. Different window functions are shown in the chapter 2. The mentioned window functions are the most employed ones in engineering researches. Erasing the edge effect results in the successful identification of cracks very close to the measurement boundaries. Hanning window function as the first tool is applied to the raw data (before wavelet transformation) set in order to reduce the edge effect. Figure 4-9 (a) illustrates the wavelet coefficients after applying Hanning window. Although, Hanning window reduces the edge effect, still there is no clear large perturbation at the crack location in the wavelet coefficients results of the windowed spatial signal. Furthermore, as shown in Figure 4-9 (a), some noises around the middle of the measurement range get more significant due to the Hanning window shape. Another

introduced function in the chapter 2 is Triangular window. This window function as the next tool is applied to the raw data set and the results are demonstrated in the Figure 4-9 (b). As it can be seen, a singularity appears at the crack location, however a few peaks in the middle of measurement area lead to misunderstanding and confusion of the crack localization. The next idea to solve the appeared problem is using more than one window function. one function is used to reduce the edge effect and the other one so as to erase the perturbations emerged because of window function shape. According to the comparison between the results in Figure 4-9, the triangular window is chosen to erase the edge effect. 1-Hanning window, which is shown in the chapter 2 (Figure 2-4) is applied to the wavelet coefficients results (after wavelet transformation with repetition number=9 and scale factor=7.4) in order to erase the emerged peaks around the middle of spatial signal. Consequently, Triangular and 1-Hanning windows are applied to the raw data and wavelet coefficients, respectively. The results are shown in the Figure 4-10. As it can be seen, a very large singularity emerges at the crack position and other peaks due to the noises are ignorable compared to it. The results prove the capability of this method in detection of a small crack close to the signal boundaries in result of effective edge effect reduction.

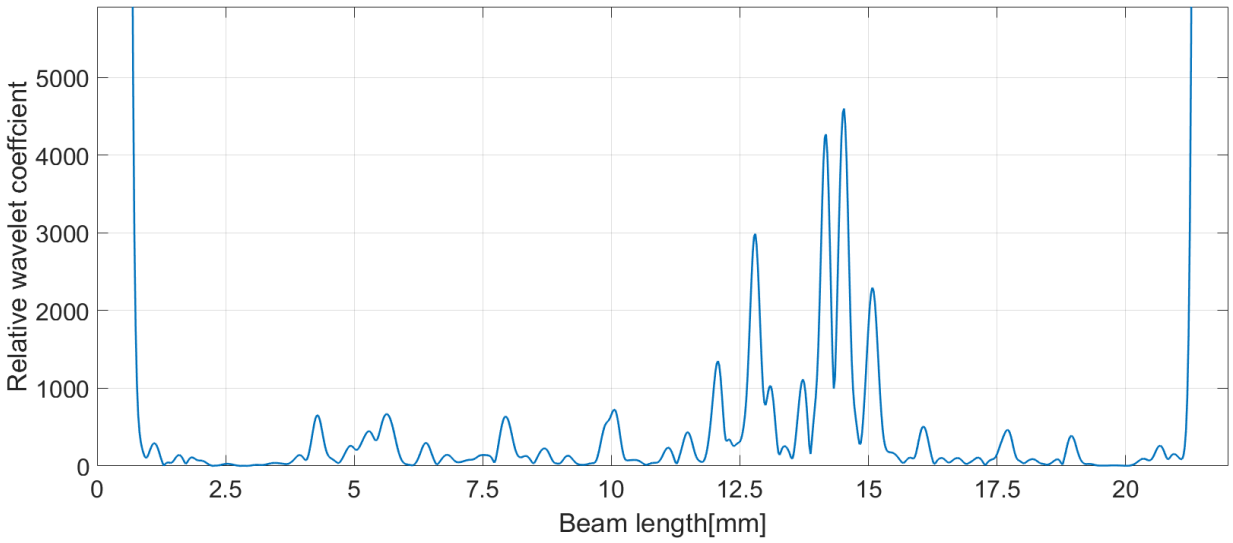

(a)

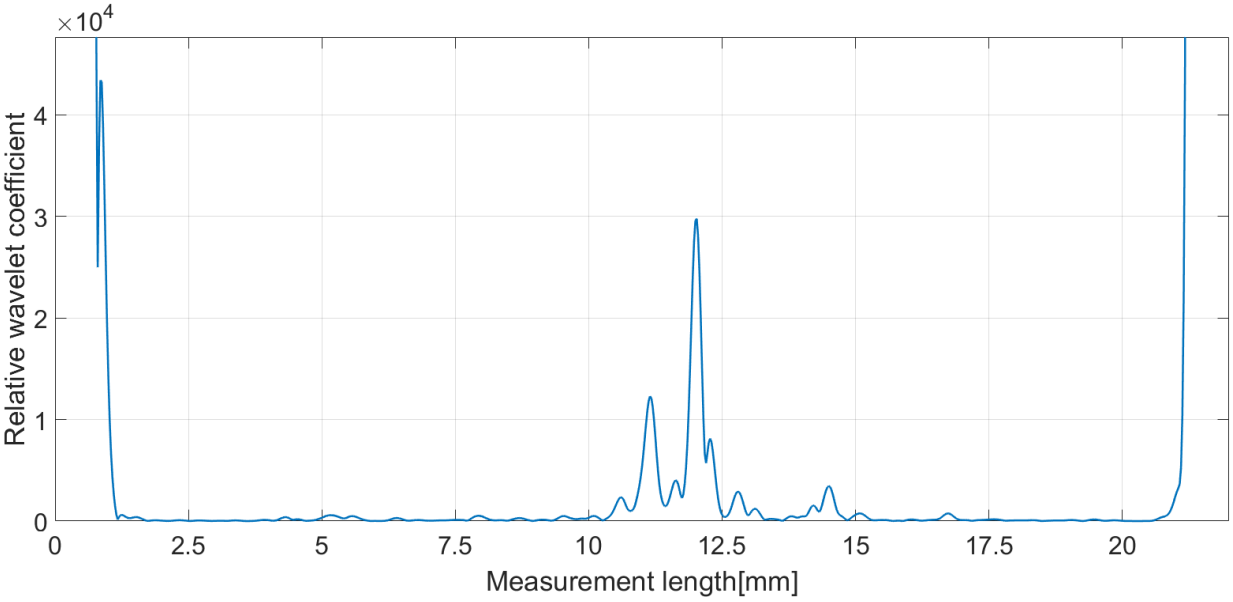

(b)

Figure 4-9 Relative wavelet coefficients along the measurement length :(a) Hanning window and (b)Triangular window have been applied to the raw data (Repetition number = 9, Scale factor = 7.4)

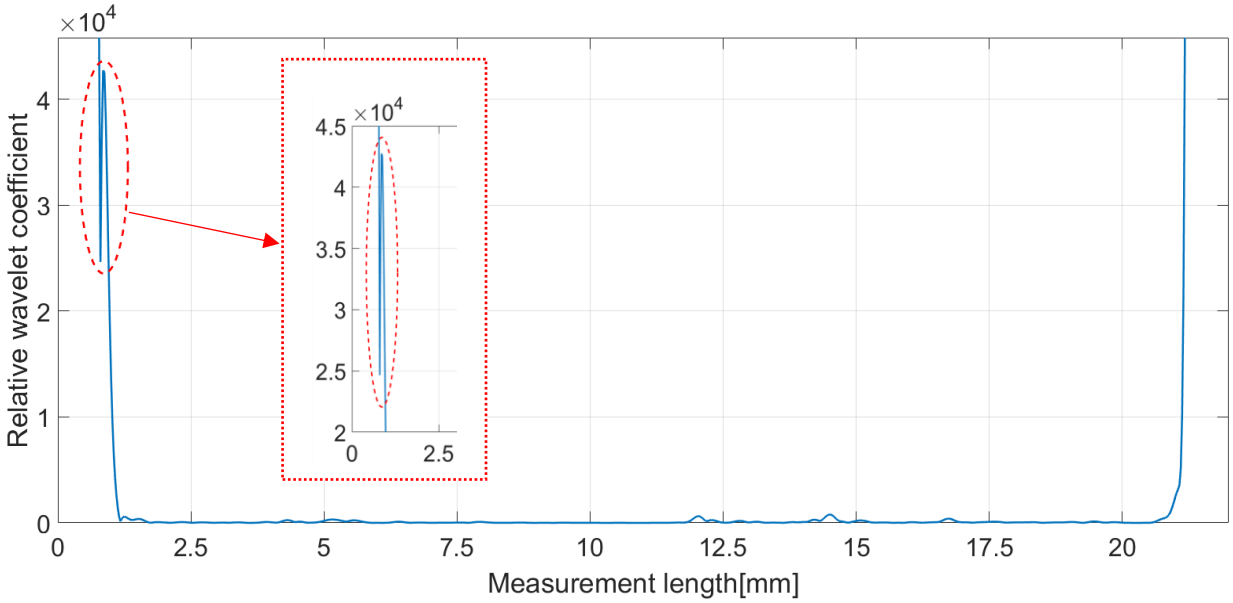

Figure 4-10 Relative wavelet coefficients along the measurement length (Triangular window has been applied to the raw data, and (1-Hann) has been applied to the wavelet coefficients) (Repetition number = 9, Scale factor = 7.4, Crack position = 0.85 mm)

5 CONCLUSIONS AND FUTURE WORKS

5.1 OVERVIEW

In this study, a high sensitive spatial wavelet-based crack localization method is presented on a cantilever beam. A brief report of the thesis procedure and main findings during our research is presented in the following paragraphs.

Firstly, a detailed theoretical model of a cracked cantilever beam is constructed. Governing equations in the modeling procedure are derived from Timoshenko theory, and a crack is represented by a torsion spring in the model. The first three mode shapes of the mathematical model are derived so as to be investigated in the simulation study. Gabor wavelet transform is employed as a tool to analyze the spatial signal of the structure, which is mode shape in the simulation study. This part of study includes the wavelet analysis, and optimization procedure for the scale factor used inside the wavelet transform. Eventually, an experimental study is performed to validate the results of the previous parts. In this part, a static displacement of a cantilever beam is obtained by a high-resolution laser. The deflection slope of the beam keeps increasing along the length direction getting away from its fixed end. This deflection slope is similar to the first mode shape slope, so the optimized scale factor range for the first mode in the simulation part is used for the investigation in the experiment.

5.2 CONCLUSIONS

Two main objectives and contributions of this research are localization of a small crack with depth of 10% of the beam height, and detection of a small crack very close to the signal boundary.

In the simulation part of this research, an optimization process is performed on the wavelet scale factor to reach higher crack locating sensitivity with spatial wavelet transformation. Optimal scale ranges with highest crack locating sensitivity for the first vibration mode is 6-8, and for the second and third ones is 5-6. Furthermore, Hanning window is employed to erase the edge effect of the wavelet transformation in order to realize the detection of cracks close to the measurement boundaries. According to simulation results, it can be concluded that by using the window function, spatial wavelet-based damage detection method is applicable even for cracks close to the both ends of the beam.

The cantilever beam is experimentally studied subjected to displacement at the free end. Such displacement curve is similar to the first mode shape of a cantilever beam. Thus, the obtained range for the scale factor in the simulation part is employed for wavelet analysis in the experiment. According to the experimental results, optimization of wavelet transformation with Gabor wavelet family and applying it to the spatial beam deflection signal show a clear improvement in the localization procedure. A crack with depth of 10% of the beam height is efficiently localized by the proposed technique. Furthermore, using proper windowing function enables this technique to detect a small perturbation caused by a crack located at 0.85 mm away from one end of the measurement range, which is covered by wavelet transform edge effect. Achieving both objectives validates this technique for detection and localization of small cracks in the structures.

5.3 FUTURE WORKS

Following points of interests can be examined in any possible continuation of this study:

1. Optimization of other wavelet families;

2. Performing the same procedure on the structures which are more complex than the beam structure (i.e. shells, and plates).

3. Experimental realization with more convenient testing equipment or methods, such as photographic method.

REFERENCES

[1] D. M. Frangopol and T. B. Messervey, “Maintenance principles for civil structures,” *Encycl. Struct. Health Monit.*, 2009.

[2] A. K. Pandey and M. Biswas, “Damage detection in structures using changes in flexibility,” *J. Sound Vib.*, vol. 169, no. 1, pp. 3–17, 1994.

[3] P. Cawley and R. D. Adams, “The location of defects in structures from measurements of natural frequencies,” *J. Strain Anal. Eng. Des.*, vol. 14, pp. 49–57, 1979.

[4] M. I. Friswell, J. E. T. Penny, and D. A. L. Wilson, “Using vibration data and statistical measures to locate damage in structures,” *Modal Anal. Int. J. Anal. Exp. Modal Anal.*, vol. 9, pp. 239–254, 1994.

[5] N. ; O. Stubbs, “Global non-destructive damage evaluation in solids,” *Int. J. Anal. Exp. Modal Anal.*, vol. 5, pp. 67–79, 1990.

[6] N. ; O. Stubbs, “Global damage detectionin solids–experimental verification,” *Int. J. Anal. Exp. Modal Anal.*, vol. 5, pp. 81–97, 1990.

[7] C. R. Farrar and G. H. James III, “System identification from ambient vibration measurements on a bridge,” *J. Sound Vib.*, vol. 205, pp. 1–18, 1997.

[8] G. Hearn and R. B. Testa, “Modal analysis for damage detection in structures,” *J. Struct. Eng.*, vol. 117, no. 10, pp. 3042–3063, 1991.

[9] W.-X. Ren and G. De Roeck, “Structural damage identification using modal data. I: Simulation verification,” *J. Struct. Eng.*, vol. 128, no. 1, pp. 87–95, 2002.

[10] M. M. F. Yuen, “A numerical study of the eigenparameters of a damaged cantilever,” *J. Sound Vib.*, vol. 103, no. 3, pp. 301–310, 1985.

[11] F. Vestroni and D. Capecchi, “Damage detection in beam structures based on frequency measurements,” *J. Eng. Mech.*, vol. 126, no. 7, pp. 761–768, 2000.

[12] C. H. J. Fox, “The location of defects in structures-A comparison of the use of natural frequency and mode shape data,” presented at the 10th International Modal Analysis Conference, 1992, vol. 1, pp. 522–528.

[13] A. K. Pandey, M. Biswas, and M. M. Samman, “Damage detection from changes in curvature mode shapes,” *J. Sound Vib.*, vol. 145, pp. 321–332, 1991.

[14] J.-T. Kim, Y.-S. Ryu, H.-M. Cho, and N. Stubbs, “Damage identification in beam-type structures: frequency-based method vs mode-shape-based method,” *Eng. Struct.*, vol. 25, no. 1, pp. 57–67, 2003.

[15] A. E. Aktan, K. L. Lee, C. Chuntavan, and T. Aksel, “Modal testing for structural identification and condition assessment of constructed facilities,” in *Proceedings-spie the International Society for Optical Engineering*, 1994, pp. 462–462.

[16] C. Surace and R. Ruotolo, “Crack detection of a beam using the wavelet transform,” presented at the PROCEEDINGS-SPIE THE INTERNATIONAL SOCIETY FOR OPTICAL ENGINEERING, 1994, pp. 1141–1141.

[17] K. M. Liew and Q. Wang, “Application of wavelet theory for crack identification in structures,” *J. Eng. Mech.*, vol. 124, pp. 152–157, 1998.

[18] Q. Wang and X. Deng, “Damage detection with spatial wavelets,” *Int. J. Solids Struct.*, vol. 36, pp. 3443–3468, 1999.

[19] N. G. Jaiswal and D. W. Pande, “Sensitizing the mode shapes of beam towards damage detection using curvature and wavelet transform,” *Int J Sci Technol Res*, vol. 4, pp. 266–272, 2015.

[20] C.-C. Chang and L.-W. Chen, “Vibration damage detection of a Timoshenko beam by spatial wavelet based approach,” *Appl. Acoust.*, vol. 64, pp. 1217–1240, 2003.

[21] C.-C. Chang and L.-W. Chen, “Detection of the location and size of cracks in the multiple cracked beam by spatial wavelet based approach,” *Mech. Syst. Signal Process.*, vol. 19, pp. 139–155, 2005.

[22] P. K. Umesha, R. Ravichandran, and K. Sivasubramanian, “Crack detection and quantification in beams using wavelets,” *Comput.-Aided Civ. Infrastruct. Eng.*, vol. 24, no. 8, pp. 593–607, 2009.

[23] S. Zhong and S. O. Oyadiji, “Crack detection in simply supported beams without baseline modal parameters by stationary wavelet transform,” *Mech. Syst. Signal Process.*, vol. 21, no. 4, pp. 1853–1884, 2007.

[24] W. Xu, M. Radzieński, W. Ostachowicz, and M. Cao, “Damage detection in plates using two-dimensional directional Gaussian wavelets and laser scanned operating deflection shapes,” *Struct. Health Monit.*, vol. 12, pp. 457–468, 2013.

[25] M. Rucka and K. Wilde, “Crack identification using wavelets on experimental static deflection profiles,” *Eng. Struct.*, vol. 28, no. 2, pp. 279–288, 2006.

[26] N. Wu and Q. Wang, “Experimental studies on damage detection of beam structures with wavelet transform,” *Int. J. Eng. Sci.*, vol. 49, pp. 253–261, 2011.

[27] Q. Wang and N. Wu, “Detecting the delamination location of a beam with a wavelet transform: an experimentalstudy,” *Smart Mater. Struct.*, vol. 20, p. 012002, 2010.

[28] M. Rucka, “Damage detection in beams using wavelet transform on higher vibration modes,” *J. Theor. Appl. Mech.*, vol. 49, pp. 399–417, 2011.

[29] M. Algaba, M. Solís, and P. Galvín, “Enhanced Modal Wavelet Analysis for Damage Detection in Beams,” in *Topics in Modal Analysis, Volume 7*, Springer, 2014, pp. 317–323.

[30] M. Solís, M. Algaba, and P. Galvín, “Continuous wavelet analysis of mode shapes differences for damage detection,” *Mech. Syst. Signal Process.*, vol. 40, pp. 645–666, 2013.

[31] D. M. Reddy and S. Swarnamani, “Damage detection and identification in structures by spatial wavelet based approach,” *Int. J. Appl. Sci. Eng. 10 1*, pp. 69–87, 2012.

[32] Z. A. Jassim, N. N. Ali, F. Mustapha, and N. A. Jalil, “A review on the vibration analysis for a damage occurrence of a cantilever beam,” *Eng. Fail. Anal.*, vol. 31, pp. 442–461, 2013.

[33] S. W. Doebling, C. R. Farrar, M. B. Prime, and D. W. Shevitz, “Damage identification and health monitoring of structural and mechanical systems from changes in their vibration characteristics: a literature review,” 1996.

[34] S. S. Rao, *Vibration of continuous systems*. John Wiley & Sons, 2007.

[35] A. Labuschagne, N. F. J. van Rensburg, and A. J. van der Merwe, “Comparison of linear beam theories,” *Math. Comput. Model.*, vol. 49, no. 1, pp. 20–30, Jan. 2009.

[36] H. Zohoor and F. Kakavand, “Vibration of Euler–Bernoulli and Timoshenko beams in large overall motion on flying support using finite element method,” *Sci. Iran.*, vol. 19, no. 4, pp. 1105–1116, 2012.

[37] R. Y. Liang, F. K. Choy, and J. Hu, “Detection of cracks in beam structures using measurements of natural frequencies,” *J. Frankl. Inst.*, vol. 328, pp. 505–518, 1991.

[38] K. Kishimoto, “Wavelet analysis of dispersive stress waves,” *JSME Int. J. Ser Mech. Mater. Eng.*, vol. 38, pp. 416–424, 1995.

[39] A. V. Oppenheim, *Discrete-time signal processing*. Pearson Education India, 1999.

[40] “Triangular window - MATLAB triang.” [Online]. Available: http://www.mathworks.com/help/signal/ref/triang.html. [Accessed: 22-Jun-2017].

[41] “Hann (Hanning) window - MATLAB hann.” [Online]. Available: http://www.mathworks.com/help/signal/ref/hann.html. [Accessed: 22-Jun-2017].

APPENDIX: LIST OF PUBLICATIONS

Published:

I. Mardasi, A. G., Wu, N., & Wu, C. (2017). High Sensitivity Crack Detection and Locating with Optimized Spatial Wavelet Analysis. *International Journal of Mechanical, Aerospace, Industrial, Mechatronic and Manufacturing Engineering*, *11*(5), 759-764.

Submitted:

I. Mardasi, A. G., Wu, N., & Wu, C. (2017). Experimental study on the localization of a small crack with optimized spatial wavelet analysis and windowing. Submitted to *Mechanical Systems and Signal Processing Journal.*